

Review

# Prospects for Anion-Exchange Membranes in Alkali Metal–Air Batteries

Misgina Tilahun Tsehaye , Fannie Alloin \*  and Cristina Iojoiu \*

Univ. Grenoble Alpes, Univ. Savoie Mont Blanc, CNRS, Grenoble INP, LEPMI, 38 000 Grenoble, France; misgina-tilahun.tsehaye@grenoble-inp.fr

\* Correspondence: Fannie.Alloin@lepmi.grenoble-inp.fr (F.A.); cristina.iojoiu@grenoble-inp.fr (C.I.)

Received: 18 October 2019; Accepted: 6 December 2019; Published: 10 December 2019



**Abstract:** Rechargeable alkali metal–air batteries have enormous potential in energy storage applications due to their high energy densities, low cost, and environmental friendliness. Membrane separators determine the performance and economic viability of these batteries. Usually, porous membrane separators taken from lithium-based batteries are used. Moreover, composite and cation-exchange membranes have been tested. However, crossover of unwanted species (such as zincate ions in zinc–air flow batteries) and/or low hydroxide ions conductivity are major issues to be overcome. On the other hand, state-of-art anion-exchange membranes (AEMs) have been applied to meet the current challenges with regard to rechargeable zinc–air batteries, which have received the most attention among alkali metal–air batteries. The recent advances and remaining challenges of AEMs for these batteries are critically discussed in this review. Correlation between the properties of the AEMs and performance and cyclability of the batteries is discussed. Finally, strategies for overcoming the remaining challenges and future outlooks on the topic are briefly provided. We believe this paper will play a significant role in promoting R&D on developing suitable AEMs with potential applications in alkali metal–air flow batteries.

**Keywords:** energy storage; alkali metal–air batteries; zinc–air batteries; anion-exchange membranes; recent advances; remaining challenges

## 1. Introduction to Alkali Metal–Air Batteries

The gradual depletion of fossil fuels and environmental concerns associated with their use have been challenging the energy sector. Thus, vast development and deployment of sustainable renewable energy sources, such as solar and wind are required [1]. Wind and solar are known to be the world’s fastest-growing energy sources [2]. Despite their economic feasibility and environmental friendliness, their intermittent nature and geographical limitations are the major challenges for their full employment as next-generation energy sources. To counteract their fluctuating energy outputs and thus improve the stability of the electrical grid, an efficient and stable electrical energy storage system is needed [3–5].

Over the years, various electrical energy storages have been identified and used. Currently, lithium (Li)-ion and lead–acid batteries are the leading energy storage technologies. Lead–acid batteries are well-established electrochemical energy storages for both automotive and industrial applications [6]. However, they have low energy density (30–50 Wh/kg), low cycling life (500–1000 cycles), and are dependent on toxic lead [7,8]. Similarly, Li-ion batteries play an important role in our daily lives, as they are the most commonly used battery in electric vehicles and electronics today. Unfortunately, their high cost per kWh and recent concerns over their safety have restricted their application, thus requiring the development of new storage technologies for the next generation [3,9,10]. The thermal runaway of the cell, which leads to whole battery pack failure, is believed to be caused by mechanical, electrical, or thermal abuses [11]. Moreover, Li-ion batteries’ energy density is only about 100–200 Wh/Kg, which

cannot provide the extended use needed for electric vehicles and large stationary applications [12]. Therefore, safe and high-energy-density energy storage systems are extremely desired. Figure 1 shows the chemistries and principal components of lead–acid and Li-ion batteries.



Figure 1. Principal components of lead–acid (left) and Li-ion (right) batteries [6].

Among several potential candidates, metal–air batteries are a promising and competitive high-energy alternative to Li-ion batteries [13]. Metal–air batteries are high energy density electrochemical cells that use air at the cathode (+ve) and metal as the anode (–ve) with an aqueous electrolyte [14]. Roughly speaking, a metal–air battery consists of four components: metal anode, electrolyte, membrane separator, and an air cathode. The metal anode can be an alkali metal (e.g., Li, Na, and K), alkaline earth metal (e.g., Mg), or first-row transition metal (e.g., Fe and Zn) [15]. The electrolyte can be aqueous (Zn–air, Fe–air, Al–air, and Mg–air) or non-aqueous (Li–air, Na–air, and K–air). Based on the electrolyte used, metal–air batteries can be classified as acidic, neutral, or alkaline [16]. As shown in Figure 2, during discharge, oxygen transforms to hydroxide ions at the cathode and metal transforms to metallic ions at the anode. The hydroxide ion functions as the main charge carrier. Figure 2 shows the main processes involved in alkali metal (Zn, Fe, Al)–air batteries, as they are the main concern of this review paper.

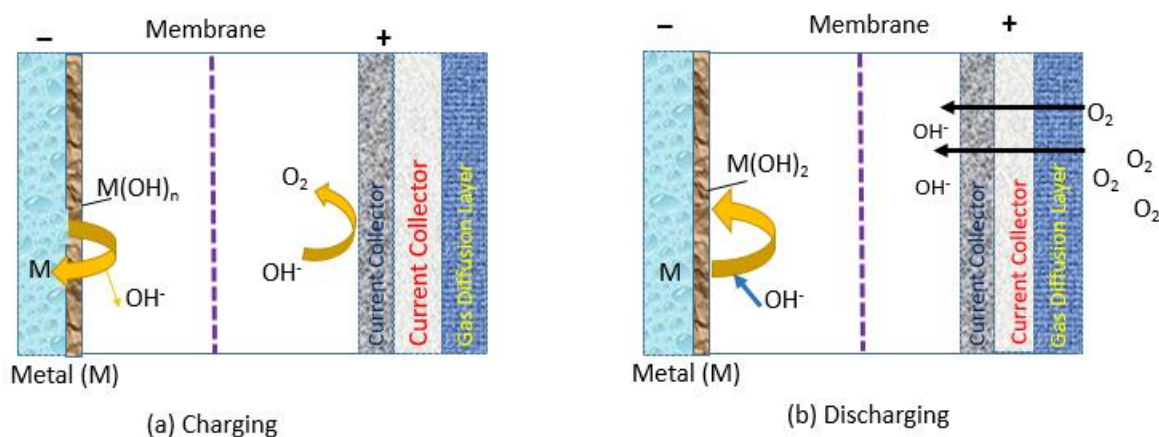


Figure 2. The main processes occurring in metal–air batteries during charge (left) and discharge (right) cycles.

Alkaline metal–air batteries (Zn–air, Al–air and Fe–air) are known to be inexpensive and non-toxic [17]. These batteries, due to their lower reactivity, easier handling, and safety, can be chosen over Li-ion batteries. Similarly, there is an intense interest in rechargeable Zn–air batteries, since Zn is the most active metal (less passive) that can be plated from an aqueous electrolyte [18]. Fe–air batteries are also very interesting as there is no dendrite formation in the negative electrode,

unlike Zn–air batteries [19]. Equally important is the fact that these batteries use the most abundant elements in the Earth’s crust, which makes them very promising as cheap energy storage devices; indeed, the elements involved, O<sub>2</sub>, Al, Fe, and Zn are the 1st, 3rd, 4th, and 24th most abundant elements in the Earth’s crust, respectively.

As shown in Table 1, due to their open configuration, the oxygen can be received from the atmosphere instead of prior incorporation, thus giving the cells high theoretical energy densities [20]. Therefore, they can be applicable across a wide range of energy transfer stations and energy storage device applications, including automotive and larger passenger vehicles and large stations for stationary application. Table 1 summarizes the reactions, nature, and characteristics of the three alkali metal–air batteries.

**Table 1.** Summarization of three alkali metal–air batteries: Zn–air, Fe–air, and Al–air batteries.

Battery Systems	Zn–Air Battery	Fe–Air Battery	Al–Air Battery
Cathode reaction		$O_2 + 2H_2O + 4e^- \leftrightarrow 4OH^-$	
Anode reaction	$Zn + 4OH^- \leftrightarrow Zn(OH)_4^{2-} + 2e^-$ $Zn(OH)_4^{2-} \leftrightarrow ZnO + H_2O + 2OH^-$	$Fe + 2OH^- \leftrightarrow Fe(OH)_2 + 2e^-$ $3Fe(OH)_2 + 2OH^- \leftrightarrow Fe_3O_4 + 4H_2O + 2e^-$	$Al + 4OH^- \leftrightarrow Al(OH)_4^- + 3e^-$
Overall reaction:	$2Zn + O_2 \leftrightarrow 2ZnO$	$3Fe + 2O_2 \leftrightarrow Fe_3O_4$	$2Al + 3O_2 \leftrightarrow Al_2O_3$
Theoretical voltage (V)	1.65	1.28	2.71
Year invented	1878	1968	1962
Cost of metals (\$US/Kg)*	2.6	0.5	1.9
Theoretical energy density (Wh/kg)	1086	764	2796
Specific Capacity (mA h/g)	820	2974	2980
Major strengths	High energy density, low cost, and environmental friendliness	-Do not form dendrites -Fourth most abundant element on the earth	-Inexpensive, safe, and is the third most abundant element in the Earth’s crust. -Significant cost savings and safety
Potential applications	Suitable for use in larger passenger vehicles	A range of applications, including automotive	Electric vehicles, military for aircraft and underwater vehicles
Remaining challenges	-Dendrite formation/growth -Bifunctional catalyst -Carbonation -Suitable membrane	Efficient and moderate-cost bifunctional -oxygen electrodes -Low-cost iron electrodes able to decrease corrosion and hydrogen evolution -New cell designs using additive manufacturing technologies	High rate of Al self-corrosion in alkaline solutions (under both open-circuit and discharge conditions)
Refs.	[5,21–25]	[19,25–27]	[14,25,28–32]

\* Data source: <http://www.metalprices.com>.

Research works on alkali metal–air batteries began earlier than those on Li-ion batteries. For instance, the first Zn–air battery was designed in 1878 (Figure 3) and commercialized in 1932 [33]. It is now one of the most common commercially available metal–air batteries worldwide [16]. On the other hand, Fe–air and Al–air batteries were developed in the 1960s [34,35]. The use of Al metal as anode material was proposed for the first time by Zaromb in 1962. However, surprisingly, despite their early beginning and becoming very promising, none are applicable for large-scale industrial deployment at the moment [15]. Among the alkali metal–air batteries, electrically rechargeable Zn–air batteries seem more likely to become commercially available any time soon. EOS Energy Storage [36], NantEnergy [37], and ZincNyx [38] are companies that recently began offering Zn–air batteries as grid energy storage systems. Moreover, many projects, such as EU-funded projects (including PowAir [39], ZAS [40] and FlowCamp [41]), are underway with the objective of achieving a low-cost, next-generation, rechargeable Zn–air flow battery. Figure 3 shows the major developments during the history of Fe–air, Al–air, and rechargeable Zn–air batteries.

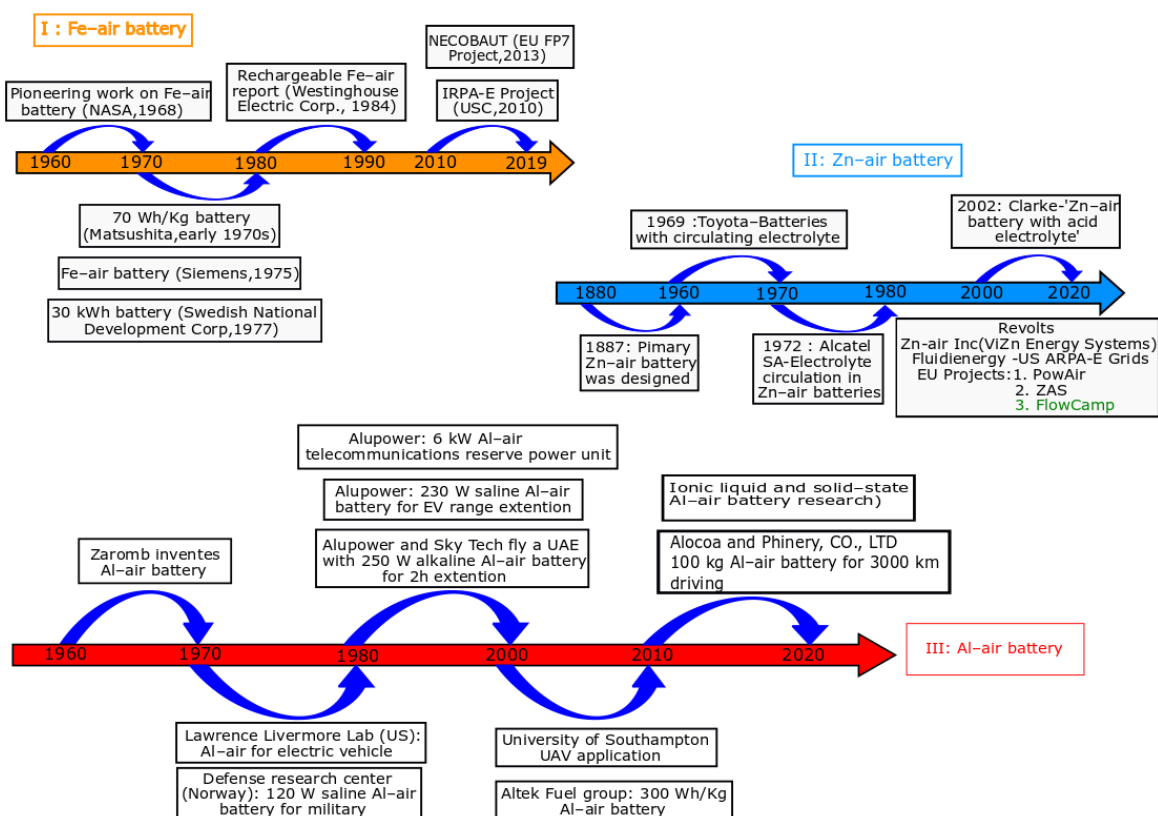


**Figure 3.** Timeline showing major developments during the history of alkali metal-air batteries: (I) Fe-air battery (adapted with permission from [19]. Copyright 2015, Wiley-VCH), (II) Zn-air flow battery [39] and (III) Al-air battery [29].

In agreement with the increase in the research devoted to these batteries in the last few years, the number of published papers has shown a steady increase, especially in the last ten years, as shown in Figure 4. It seems that in recent years, there has been significant research effort and progress with regard to the development of alkali metal-air batteries. In particular, the number of papers published on Zn-air and Fe-air batteries has shown a steady increase in the past 10 years (2011–2019). There were only a few papers published in the years before that (2000–2010, not included in the graph) in all of these batteries. Among the three, Zn-air and Fe-air batteries seem to have higher research activities compared to Al-air batteries, in terms of the number of published papers.

However, despite their early beginning and being active research topics, their development and commercialization have been hampered by several remaining challenges associated with their components, such as the metal anode (corrosion, forming passivation layers, dendritic formation, electrode deformation, and energy loss due to self-discharging), air cathode (lack of efficient catalysts for both oxygen reduction and evolution reactions, affecting electrolyte stability, and gas diffusion blockage by side reaction products), and electrolyte (side reaction with the anode, reaction with  $\text{CO}_2$  from the air, and low conductivity) [15,18] (Table 1). These problems have been well studied and reviewed in the literature [22,42,43]. As a result of the low shelf-life and cell irreversibility of the batteries, especially for Fe-air and Al-air batteries, they still remain in the early stages of development [20,31,44].

Another challenge is the lack of a suitable membrane for the batteries. The main roles of membrane are  $\text{OH}^-$  ion transportation, avoiding mixing and short-circuit, blocking unwanted species crossover (zincate ( $\text{Zn}(\text{OH})_4^{2-}$ ) ions in Zn-air battery), and dendrite growth suppression [45]. The membrane would act as a conductor for the  $\text{OH}^-$  ions as well as a separator for the electrolyte solution. Different membrane separator types, such as organic polymer porous membranes, inorganic membranes [46], composite membranes [47], cation-exchange membranes [48], and anion-exchange membranes (AEMs) [49] have been used in Zn-air battery applications.

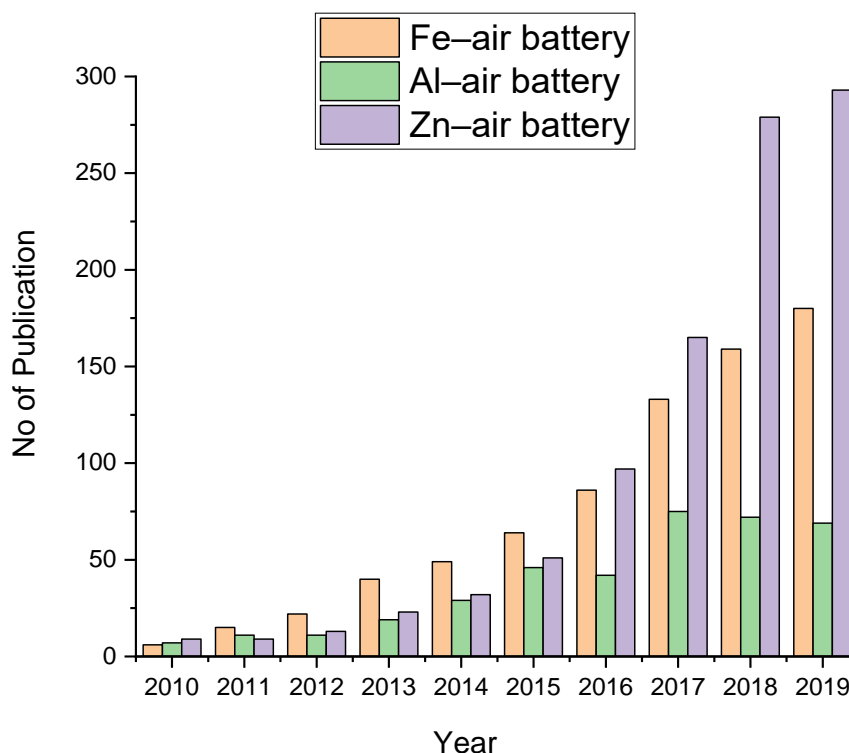


**Figure 4.** Number of publications per year regarding Zn-air batteries, Al-air batteries, and Fe-air batteries as derived from Web of Knowledge (Last checked on October 08, 2019).

Commercial Zn-air batteries commonly use laminated separators (typically Celgard<sup>®</sup>5550), which is a porous polyolefin separator.  $\text{Zn}(\text{OH})_4^{2-}$  ion crossover due to their open structure has been reported to be the main drawback associated with the use of such porous membrane separators. This gives rise to an increase in cell polarization and loss of capacity with cycling [45]. This clearly indicates the substantial need to control the  $\text{Zn}(\text{OH})_4^{2-}$  ion crossover [50]. To minimize this problem, techniques such as filling pores with inorganic particles (composite membrane) [47] and coating with anion-selective polymers have been employed [50]. The former has been reported to significantly increase the membranes' resistance (applying 0.3 g  $\text{Mn}(\text{OH})_2$  on one or two 10  $\text{cm}^2$  Celgard<sup>®</sup>3401 resulted in resistance three orders of magnitude larger), while the latter has not yet been well explored.

To completely solve the problem, the use of AEMs that are selective to the passage of  $\text{OH}^-$  ions has been widely recommended [25,45]. Various advantages can be mentioned from using AEM in alkali metal-air batteries, especially in Zn-air batteries: (i) minimizing or avoiding zincate ion permeation toward the air electrode, (ii) reducing the tendency to form and shape change of dendrites, and (iii) preventing leaching of catalysts from the air electrode to the Zn electrode. Moreover, the ion exchange membrane may also help to prevent the breakdown of the air electrode and to assist in the maintenance of a stable three-phase boundary at the air electrode [51–53].

The use of AEM as a separator in these systems is analogous to the famous use of Nafion<sup>®</sup> (and other cation-exchange membranes) in vanadium redox flow batteries, in which  $\text{VO}_2^+/\text{VO}^{2+}$  and  $\text{V}^{3+}/\text{V}^{2+}$  serve as positive and negative redox couples, respectively, separated by an ion-exchange membrane [54–57]. The well-designed, defined nanochannel morphologies of Nafion<sup>®</sup> enable it to have high proton conductivity, whereas the selectivity of the membrane is controlled by the size of the nanochannel. Furthermore, to reduce the possible permeation of  $\text{VO}^{2+}$  and increase the ion selectivity of Nafion<sup>®</sup>, various modification methods, including composite membranes, have been proposed [58,59].

On the other hand, even though the promise of AEMs for Zn-air batteries was identified a long time ago, it remains a surprisingly underinvestigated topic to date, despite the wide recommendations

and huge potential. As a result, it remains almost unclear whether AEMs can be used practically in the long term in alkali metal–air batteries [60]. On top of that, there are only a few companies providing robust AEMs with potential applications in an alkaline environment, and there is not much information available in the literature with regards to most of these membranes' practical applications in alkali metal–air batteries.

In this review paper, we address the recent advances and remaining challenges (and strategies to solve them) of AEMs in alkali metal–air batteries, mainly Zn–air batteries, which have received the most attention. However, it should be noted that similar performance and challenges can be expected by applying AEMs in other alkali metal–air batteries. The review is divided into three parts. First, recent advances in AEMs for zinc–air batteries are discussed. Next, the remaining current challenges of AEMs and strategies to solve these problems are provided. In the end, we present a summary and outlooks on the topic.

## 2. Advances in AEMs for Alkali Metal–Air Batteries

A literature survey was done and analyzed to understand the weaknesses and strengths of the AEMs reported in the literature and commercial AEMs, such as A201<sup>®</sup> (Tokuyama Corporation, Japan) and FAA-3<sup>®</sup> (FumaTech, Germany) when used in alkali metal–air batteries. FAA<sup>®</sup>-3 is a slightly cross-linked, non-reinforced AEM consisting of a polyaromatic backbone with a quaternary ammonium group. FAA<sup>®</sup>-3-50 is 45–55  $\mu\text{m}$  thick and has an ion-exchange capacity (IEC) of 2 meq/g in chloride form [61–63]. A201<sup>®</sup> (IEC = 1.7 mmol/g and 28  $\mu\text{m}$  thick) employs quaternary ammonium groups and hydrocarbon main chain [64,65] AEMs used in Zn–air batteries are mainly discussed, as these batteries are better explored compared to the others. Among the commercial AEMs, A201<sup>®</sup> membrane has been most tested in rechargeable Zn–air batteries. Moreover, in addition to commercial AEMs, preparation of AEMs for Zn–air batteries has been reported in the literature. The cycling stabilities of the batteries have been found to be dependent on ionic conductivity, zincate diffusion (selectivity), water uptake capacity, and anisotropic swelling ratio of the membranes. Anisotropic swelling of membranes is defined as the ratio of through-plane to in-plane swelling of the membrane. Moreover, prospects on the possible use of other commercial AEMs have also been investigated.

Recently, Abbasi et al. [66] prepared poly (p-phenylene oxide) (PPO)-based AEMs using three different cations—trimethylamine (TMA), 1-methylpyrrolidine (MPY), and 1-methylimidazole (MIM)—and tested them in a Zn–air battery. PPO-TMA and PPO-MPY exhibited low zincate diffusion coefficients ( $1.13 \times 10^{-8}$ , and  $0.28 \times 10^{-8}$   $\text{cm}^2/\text{min}$ , respectively) and high discharge capacity (about ~800 mAh/g<sub>Zn</sub> using PPO-TMA). The PPO-TMA membrane was reported to have low conductivity (0.17 mS/cm) despite its high water uptake (89 wt.%). On the other hand, the membranes showed good alkaline stability in a solution typically used in Zn–air batteries (7 M KOH solution at 30 °C) for at least 150 h. Moreover, PPO-TMA showed good electrochemical stability in a range of –1.5 to +1.5 V (stability window of 3 V). It is a well-established fact that PPO-TMA membranes undergo an S<sub>N</sub>2 hydroxide attack [67]. In this degradation process, the C–N bond electrons move towards the nitrogen while the OH<sup>–</sup> forms a new bond with the  $\alpha$  carbon, producing trimethylamine and benzyl alcohol. Therefore, the relative alkaline stability of the current membranes could be due to the low temperature and the reasonable duration of the test.

In another study, a polysulfonium-cation-based AEM was fabricated and used in a Zn–air battery [49]. Compared to Celgard<sup>®</sup> 5550, the prepared membrane demonstrated better ionic selectivity. As a result, the capacity was 6-fold higher than that of reference membrane during discharge. However, the species crossing over was mistakenly considered to be Zn<sup>2+</sup>, rather than Zn(OH)<sub>4</sub><sup>2–</sup>. Moreover, the cyclability of the battery was not studied.

A porous alkaline-exchange membrane based on quaternary ammonium (QA)-functionalized nanocellulose (2-QAFC, cellulose nanofibres modified with 200 mol. % concentration of dimethyloctadecyl [3-(trimethoxysilyl) propyl] ammonium chloride) exhibiting high hydroxide ion conductivity (21.2 mS/cm) and water swelling (95.6%) was developed [68]. Figure 5 presents the

procedure followed for the preparation of the 2-QAFC membrane (Figure 5a), galvanostatic discharge of solid-state Zn–air batteries using the 2-QAFC, A201<sup>®</sup> and KOH-PC membranes (1 M KOH-doped pristine cellulose membranes) (Figure 5b), and galvanostatic charge and discharge cycling (Figure 5c). Both the prepared 2-QAFC (30  $\mu\text{m}$  thickness) and commercial A201<sup>®</sup> membranes (28  $\mu\text{m}$  thickness) were tested in a flexible, solid-state rechargeable Zn–air battery. Initially, the A201<sup>®</sup>-based battery had a higher discharge voltage; however, it was quickly surpassed by the 2-QAFC-based battery, showing a voltage plateau about 180 mV higher and a higher discharge capacity.

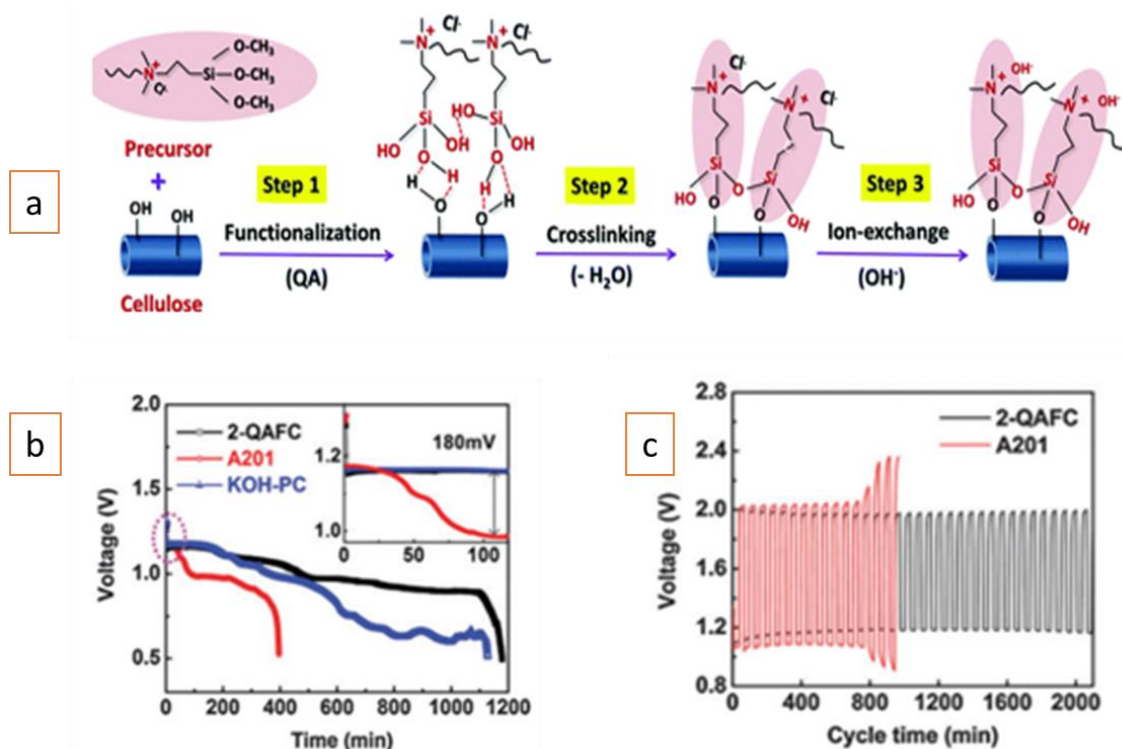


**Figure 5.** (a) Schematic diagram of the chemical structure evolution of the nanocellulose membrane by functionalization, cross-linking, and hydroxide exchange. (b) Galvanostatic discharge of solid-state Zn–air batteries using the 2-QAFC, A201<sup>®</sup>, and KOH-PC membranes at a current density of 25 mA/g. (c) Galvanostatic charge and discharge cycling of the 2-QAFC and A201<sup>®</sup> membranes at a current density of 250 mA/g with a 60 min per cycle period. Reprinted with permission from Reference [68]. Copyright 2016, Royal Society of Chemistry.

The A201<sup>®</sup>-based battery exhibited a rapid voltage and capacity loss, which could have been due to the progressive loss of water and ionic conductivity in the membrane during the constant current applied. It seems that water consumption during oxygen reduction in air electrode leads to electrolyte drying problems and a shortened battery life. Since water plays an important role in the ion transport, its loss can directly reduce ionic transport limitation inside the air electrode (decrease of the OH<sup>-</sup> mobility, degrading the catalyst/electrolyte interface) and inside the membrane, resulting in a large ohmic polarization of the battery. Nevertheless, it must be noted that by wetting the membrane with distilled, de-ionized water, it is possible to regenerate the performance of the battery. As a consequence, the A201<sup>®</sup>-based battery deteriorated after a few cycles (Figure 5c), showing large discharge and charge polarizations.

On the other hand, the 2-QAFC-based battery exhibited superior cycling stability in both the charge and discharge (Figure 5c). This superior cycling stability was assumed to be due to the battery's holding a higher amount of water (95.6%, OH<sup>-</sup> form) and having a smaller anisotropic swelling ratio (1.1) of 2-QAFC than A201<sup>®</sup> membrane (44.3% water uptake and 4.4 anisotropic swelling ratio). In other

words, the 2-QAFC membrane could tolerate the periodic stress and dehydration during the discharge and charge processes.

Similarly, a QA-functionalized, crosslinked nanocellulose/graphene oxide (QAFCGO) membrane was prepared and assembled in a flexible rechargeable Zn–air battery [69]. Batteries employing the QAFCGO and A201<sup>®</sup> membranes exhibited similar high open-circuit voltages ( $\approx 1.4$  V). The QAFCGO-based battery showed a better performance compared to the A201<sup>®</sup>-based battery, with smaller over potentials for both discharge and charge processes. At high current densities (above 20 mA/cm<sup>2</sup>), the QAFCGO-based battery showed a remarkable advantage over the A201<sup>®</sup>-based battery (Figure 6a). As shown in Figure 6b, the QAFCGO-based battery exhibited much higher cycling stability performance than that of A201<sup>®</sup>-based battery. Furthermore, the former battery had higher peak power density (44.1 mW/cm<sup>2</sup>) than the latter (33.2 mW/cm<sup>2</sup>) (Figure 6c).

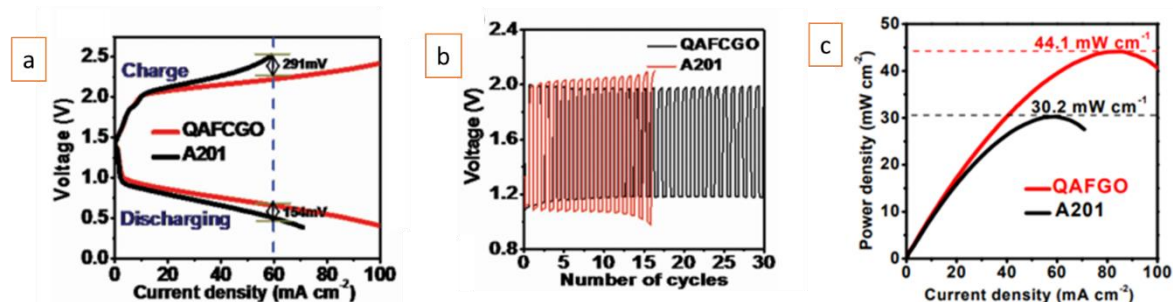


**Figure 6.** QAFCGO- and A201<sup>®</sup>-membrane-based Zn–air batteries: (a) charge and discharge polarization curves, (b) galvanostatic charge and discharge cycling at a current density of 1 mA/cm<sup>2</sup> with a 20 min per cycle period (10 min discharge followed by 10 min charge), and (c) the power density plots at a current density of 1 mA/cm<sup>2</sup>. Reproduced with permission from Reference [69]. Copyright 2016, Wiley-VCH.

Similarly to the finding of Fu et al. [68], the A201<sup>®</sup>-based battery showed a clear performance decline (with large charge and discharge polarizations) after relatively few cycles (Figure 6b). On the other hand, the QAFCGO-based battery was reported to continue without any sign of performance loss after 30 cycles. As clearly noted previously, the superior cyclability and performance stability of the QAFCGO-based battery compared to the A201<sup>®</sup>-based battery was attributed to the QAFCGO membrane's higher water uptake (5 times higher than that of the A201<sup>®</sup> membrane) and smaller anisotropic swelling degree (half of that of the A201<sup>®</sup> membrane).

Furthermore, AEMs composed of both cross-linked chitosan (CS) and poly (diallyldimethylammonium chloride) (PDDA) and A201<sup>®</sup> membranes were tested in all-solid-state Zn–air batteries [60] (Figure 7a). The prepared CS-PDDA membrane exhibited high OH<sup>−</sup> conductivity (24 mS/cm), strong alkaline stability (216 h at 8 M KOH), and a low degree of anisotropic swelling (1.7), all of which are very important membrane properties required for long-term and superior electrochemical performance in all-solid-state Zn–air battery. The CS-PDDA-based battery exhibited a high open-circuit voltage (1.3 V) and superior peak power density to the A201<sup>®</sup>-based cell (48.9 vs. 41.4 mW/cm<sup>2</sup>) under the same measurement conditions (Figure 7b). Additionally, the CS-PDDA-based battery initially had a higher discharge voltage (1.14 vs. 1 V), and exhibited lower discharge and charge polarization and longer cycle times (even if only a few cycles were shown) than the battery with the commercial A201<sup>®</sup> membrane (Figure 7c,d).

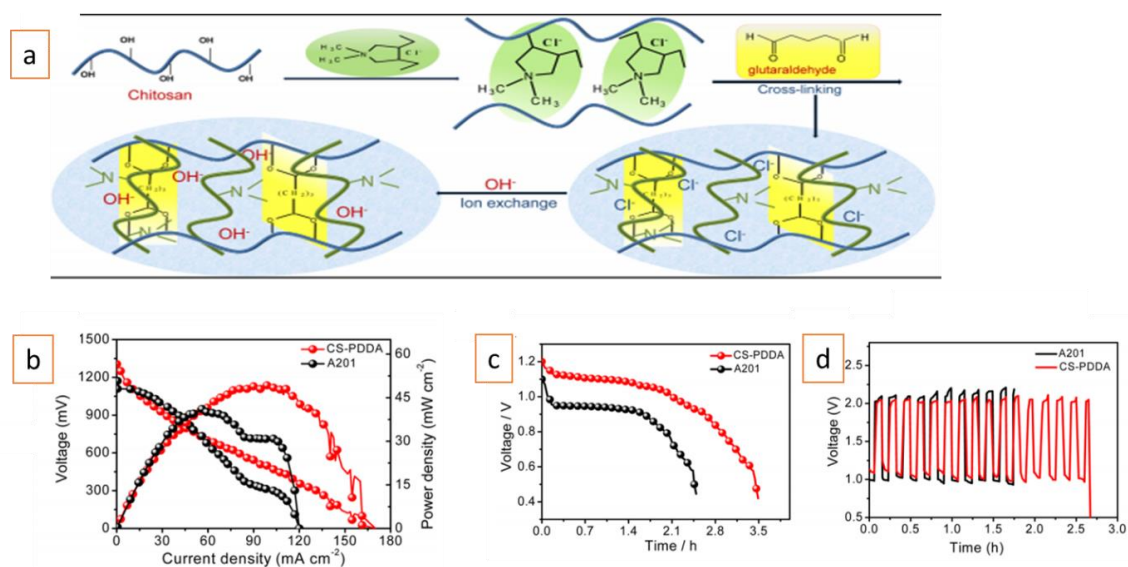


**Figure 7.** (a) Schematic diagram of the overall preparation procedure for the CS-PDDA-OH<sup>-</sup> membrane; (b) polarization curve and corresponding power density plots; (c) galvanostatic discharge of the batteries; (d) galvanostatic charge and discharge cycling of the batteries using the CS-PDDA-OH<sup>-</sup> and A201<sup>®</sup> membranes at 3 mA/cm<sup>2</sup> with 10 min per cycle period. Adapted with permission from Reference [61]. Copyright 2018, American Chemical Society.

As mentioned in previous studies [69,70], the superior performance of the prepared membrane over A201<sup>®</sup> was due to its smaller anisotropic swelling and higher water uptake (4 times higher water uptake than the A201<sup>®</sup> membrane). It should be noted that the anisotropic swelling ratio of commercial A201<sup>®</sup> membrane was different in all the studies, indicating the lack of a standardized testing protocol.

Moreover, in addition to polysulfonium and QAs, imidazolium cations have been used to prepare AEMs for Zn–air batteries. Zarrin et al. [70] prepared a graphene oxide membrane functionalized with 1-hexyl-3-methylimidazolium chloride molecules (HMIM/GO) with potential for wearable electronics, including flexible Zn–air batteries. The prepared 5-HMIM/GO (5 refers to weight ratio of HMIM to GO, 27  $\mu\text{m}$ ) and A201<sup>®</sup> membranes were tested in flexible Zn–air batteries. The 5-HMIM/GO membrane was reported to have a hydroxide conductivity of 44 mS/cm at room temperature and 30% relative humidity. Both membranes exhibited stable charge/discharge performances for 60 cycles. The 5-HMIM/GO-membrane-based flexible Zn–air battery exhibited a charge–discharge voltage polarization at low relative humidity and room temperature that was comparable to that of A201<sup>®</sup>-based battery in a humidified environment. This was attributed to the high rate of ion transfer of the former membrane in the studied conditions.

All in all, all the presented studies indicate the need for development of an alkaline AEM with high hydroxide conductivity (at room temperature) and smaller anisotropic swelling degree. It can be concluded that the A201<sup>®</sup> membrane may not be practical for long-term rechargeable Zn–air batteries; in the studied systems, it was reported that its performance began to deteriorate after only a few hours. Therefore, in addition to preparing new, high-performing AEMs, testing other commercially available AEMs should be done to understand and determine their potential applications in such batteries.

Alkaline AEMs from Fumatech BWT GmbH (typically, fumapem<sup>®</sup> FAA and fumasep<sup>®</sup> FAP) are suggested by the company to be suitable separators for Zn–air batteries [71]. However, there have not been many studies in the literature to date about their practical use. Anion-exchange polymer (AEP) resin (FAA<sup>®</sup>-3-SOLUT-10 in NMP, Fumatech BWT GmbH) was used to prepare a separator and used as the separator to prepare transparent, bendable secondary Zn–air batteries [72]. The membrane was prepared using a solution (10% of AEP solution) casting method. The produced battery exhibited a maximum power density of 9.77 mW/cm<sup>2</sup>. The cells were reported to be stable for at least 100 cycles. In another study, a fumatech<sup>®</sup>-FAA membrane doped with KOH was used to prepare the

membrane electrode assembly for a Zn–air battery [73]. The battery exhibited a peak power density of 170 and 164 mW/cm<sup>2</sup> based on Fe-LC-900 (FeCl<sub>3</sub>–leather, pyrolysis temperatures of 900 °C) and Pt/C-catalyst-based air electrodes, respectively. However, in both studies, not much information was providing regarding the effects, weakness, and strength of the membranes used.

According to the technical datasheet provided by the company, fumapem<sup>®</sup> FAA-3-50 membrane, in its OH<sup>−</sup> form, has 40 wt. % H<sub>2</sub>O uptake and a dimensional swelling (in H<sub>2</sub>O) of 17% at 25 °C [74]. The membrane's in-plane swelling ratio, and thus anisotropic swelling ratio, has not been reported to date. All in all, considering its relatively low water uptake, low performance can be expected. This is due to potential periodic stress and dehydration of the membrane, similarly to A201<sup>®</sup> membrane. However, testing in a real system is the only way to observe and understand its real strengths and weaknesses.

### 3. Overcoming the Remaining Challenges

Over the years, there has been a lot of progress and improvements regarding the development stable and conductive AEMs. AEMs that are highly conductive, especially at high temperatures, have been reported [75,76]. There have also been promising improvements on the alkaline stability of such membranes. However, a suitable high-performing, alkali-stable AEM is still not available commercially. There are some challenges affecting the performance and lifespan of AEMs in alkali metal–air batteries that remain to be solved. Low alkaline stability and hydroxide conductivity of current AEMs remain significant problems [77]. The high production cost of the membranes will remain a very important aspect determining the feasibility for large-scale and industrial applications. Lack of a standardized protocol for testing AEMs is another critical issue that needs to be addressed. Last but not least, the lack of high-performing suitable AEMs that have been specifically prepared for this application (alkali metal–air batteries) limits the potential applications of AEMs in those batteries. In this section, a discussion on these problems and the strategies for minimizing or avoiding them is provided.

#### 3.1. Low Alkaline Stability of Current AEMs

One of the main challenges of applying AEMs in Zn–air batteries, similarly to alkaline fuel cells, is their limited alkaline stability. It is a well-established fact that both the polymer backbone and cation play an important role in determining the stability/degradation of AEMs. The nucleophile hydroxide ion is able to degrade both the cation and the polymer backbone. Moreover, the spacer between them, when used, has been reported to play an important role depending on its chemical nature and length. In practice, the cation is the weakest point of degradation. For this reason, it has received the most attention.

As discussed in Section 2, various cation group types, including QA [78–80], imidazolium [81,82], phosphonium [83,84], and guanidinium [85,86] have been used for preparing AEMs. Among them, QAs are the most frequently used because they are not only easy to prepare, but also easier to attach to the polymer backbone. The common degradation mechanisms of QA, imidazolium, and phosphonium are provided in Figure 8. Hofmann elimination and substitution at the benzylic carbon and at the  $\alpha$  carbon are among the most common degradation pathways for most QA-based AEMs.

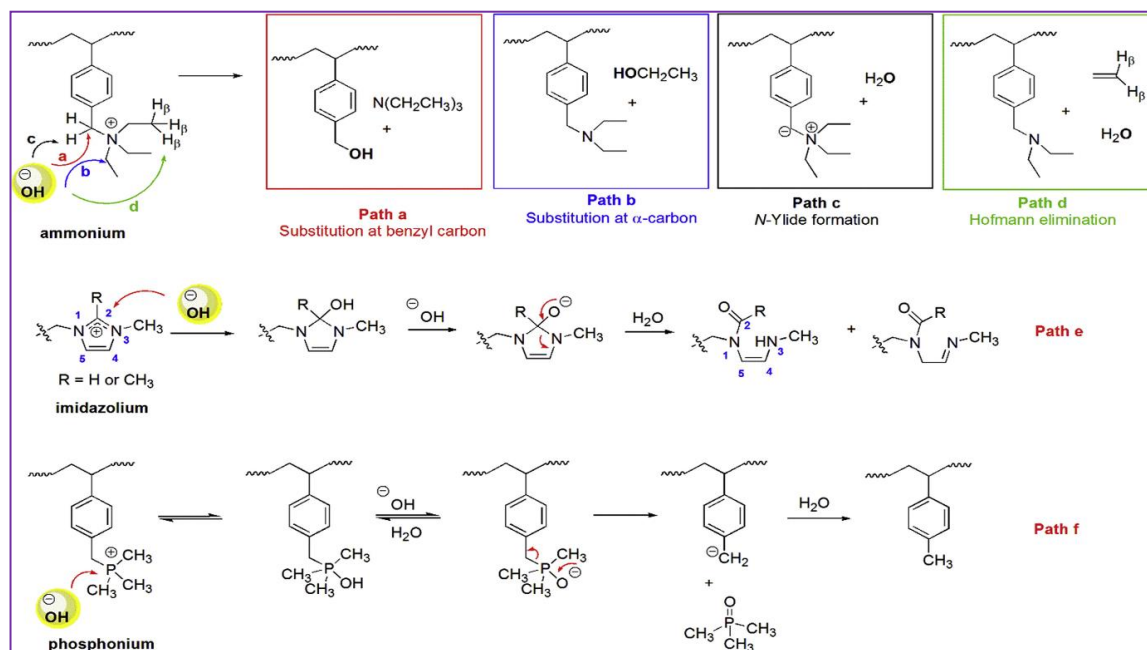


**Figure 8.** Degradation mechanisms of cations: quaternary ammonium, imidazolium, and phosphonium. Taken with permission from Reference [87]. Copyright 2017 Elsevier.

Considering the common degradation mechanisms of the cations, it is therefore important to minimize or avoid these weak points in order to develop a cation with better stability. To achieve this goal, various strategies have been proposed and employed. The most typical way to minimize alkaline chemical degradation is to prepare AEMs resistant to the Hofmann elimination by preparing AEMs without hydrogen at the  $\beta$  position to the quaternary nitrogen [88] (Figure 9, strategy I). This strategy helps to avoid the degradation path in Figure 8 path d.

Another technique that has been employed is to avoid  $S_N2$  reactions (substitution at  $\alpha$  carbon, Figure 8 path b) is to put the cation far away from the polymer backbone by introducing a spacer chain between them. Poly(phenylene)-based AEMs carrying hexamethylene-trimethylammonium have shown much better stability than membranes containing benzyl-trimethylammonium (BTMA) (5% vs. 33% conductivity loss after immersion in 4 M KOH at 90 °C for 14 days) (Figure 9, strategy II) [89]. Similarly, Jannasch [90] reported both the conductivity and alkaline stability of the membrane to be significantly enhanced by placing the cationic groups on flexible and hydrolytically stable alkyl spacers. The long-chain spacers are believed to provide steric strain for inhibition of the Hofmann elimination reaction [91].

Furthermore, incorporating a long-chain spacer between the polymer backbone and the cation has been found to enhance the microphase separation between the hydrophilic and hydrophobic domains [92], which have been reported to play a vital role in determining the rate of AEM degradation. Morphology in AEMs, like phase separation, can improve the chemical stability because it induces separation between the hydrophobic domains that support mechanical and chemical stabilities, while the interconnected hydrophilic domains transport ions. This way, the nucleophilic sources stay in the hydrophilic domain, and the hydrophobic domains thus become less susceptible to chemical attack [93]. Moreover, with an increasing number of water molecules solvating the hydroxide, its nucleophilicity and basicity are hindered, and the QA degradation is significantly slowed. This is due to the fact that the reactivity of  $\text{OH}^-$  is dependent not only on the temperature, but also on the water concentration. Therefore, with the right amount of water and at low temperatures, even QA salts considered less or unstable present significantly improved lifetimes [94,95] (Figure 9, strategy III).

Heterocyclic and spirocyclic ammonium molecules have been found to have improved alkaline stability compared with the more typical tetraalkylammonium and imidazolium compounds [91].

In one study, spirocyclic 6-azonia-spiro [5.5] small undecane molecules showed the highest stability in alkaline medium (110 h half-life at 160 °C and 10 M NaOH) among the investigated species (Figure 9, strategy IV). The chemical stability of these cations against Hoffman elimination and ring-opening reaction is believed to be due to the geometric constraints of the ring on the transition state. Therefore, the development of water-insoluble AEM materials containing N-spirocyclic ammonium groups is an interesting prospect. However, attaching those molecules into the polymer backbone is a challenge. As a result, there are currently only a few AEMs prepared using heterocyclic and spirocyclic molecules [96–98]. Strasser et al. [96] prepared promising AEMs by copolymerizing the end-functionalized polydiallylpiperidinium oligomers with polysulfone monomers. The membranes were reported to maintain 92% of their conductivity after 5 days in 1 M KOH at 80 °C. Moreover, Jannasch et al. [97] prepared water-insoluble, transparent, and mechanically robust AEMs using PPO as the polymer backbone and N-spirocyclic ammonium groups. However, the alkaline stability of this membrane was not studied.

Free-radica- initiated cyclopolymerization has been used with diallyl ammonium halides. This method is expected to extend to allylmethallyl and dimethallyl ammonium halides as well [99]. These ammonium halides are expected to have a higher degree of alkaline stability, since Hoffman elimination is not expected to happen. However, using this method, the monomer incorporation to the polymer backbone degree may not be high or efficient enough. Instead, another method with potential applications is UV-initiated polymerization at elevated temperatures, which could be used to obtain AEMs bearing diallyl, allylmethallyl, and dimethallyl ammonium halides [99].

The synthesis of cationic polyelectrolytes which are sterically protected around the C2 position is another promising technique for the preparation alkaline stable cations. The stability of benzimidazolium-based AEMs was greatly enhanced by introducing a bulky moiety at the labile benzimidazolium C2 position [100]. Holdcroft et al. [101] synthesized poly(arylene-imidazoliums) by microwave polycondensation of dialdehyde with bisbenzyl and quantitatively functionalized by alkylation. The cationic polyelectrolyte was determined to be stable in 10 M KOH (aq) at 100 °C ( $t_{1/2} > 5000$  h) (Figure 9, strategy V). The five methods discussed to develop alkaline stable cations, and thereby membranes, are summarized in Figure 9.

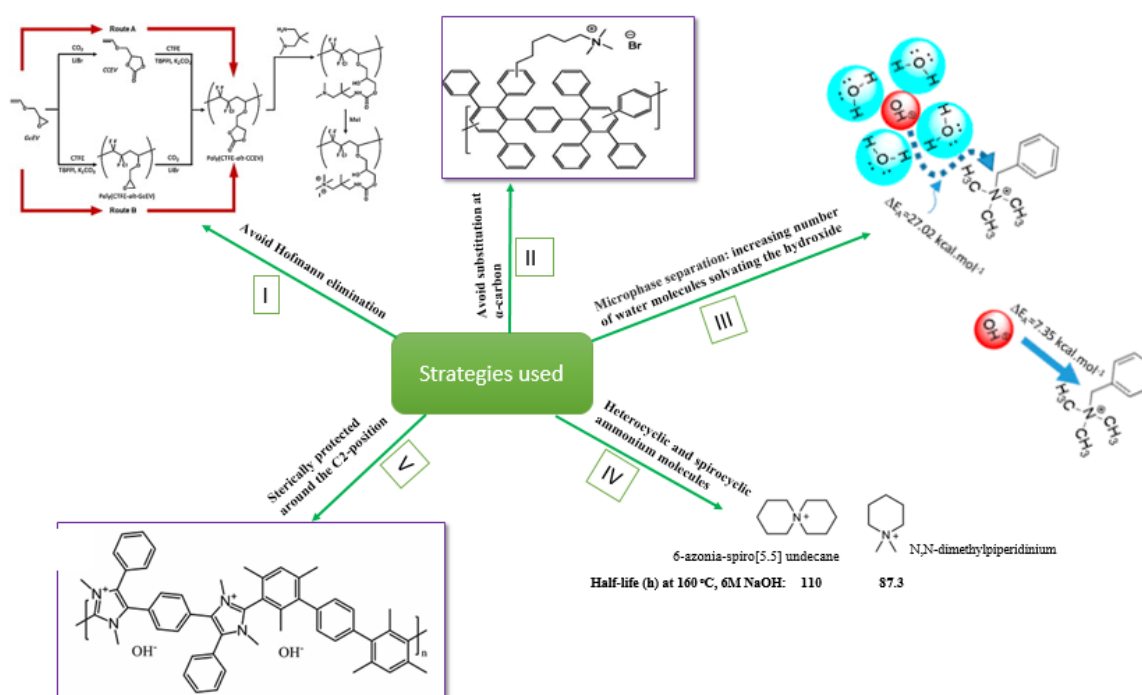
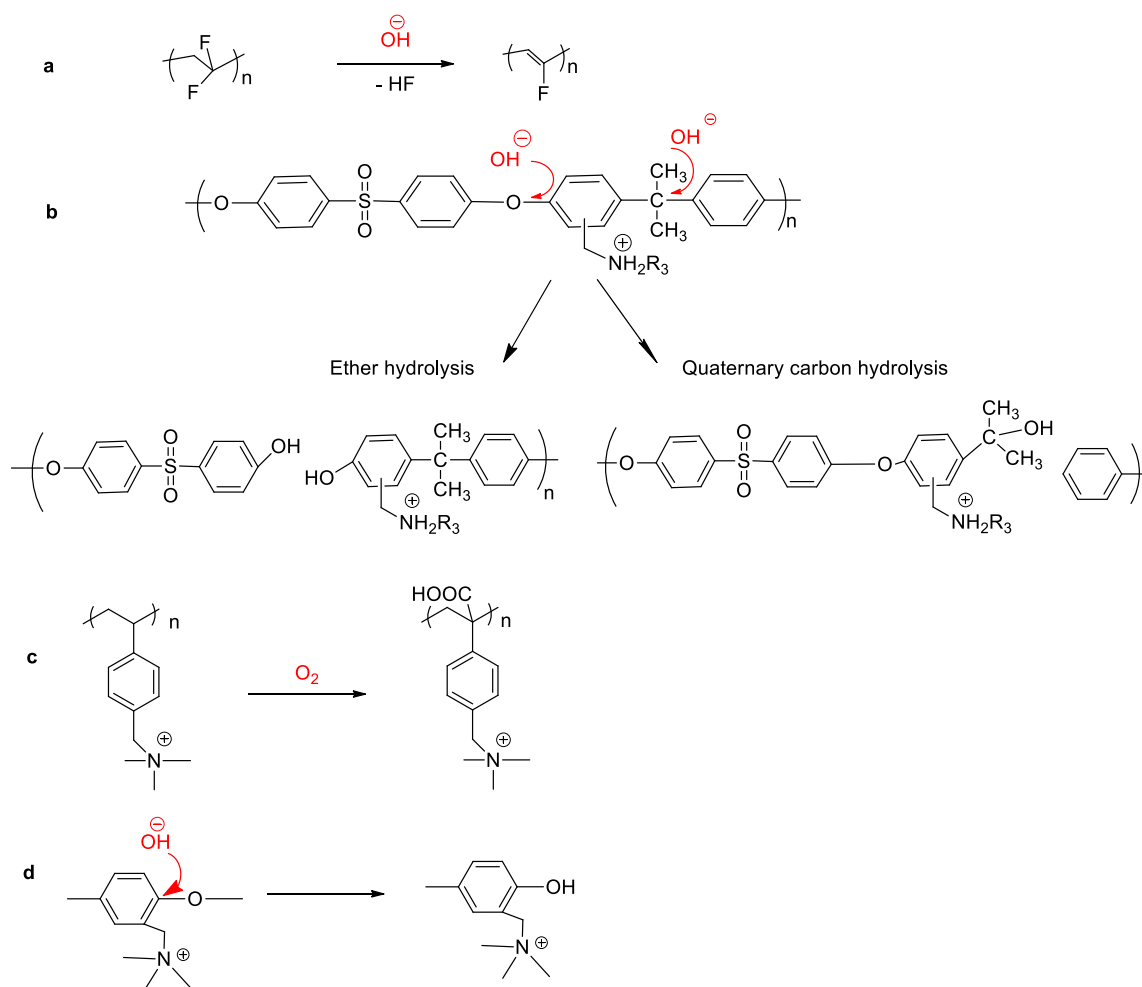


Figure 9. General strategies used for preparing alkaline stable cations [88,89,91,95,101].

All in all, there has been a lot of progress with regard to stability improvement of AEMs. Relatively improved alkali stable cations have been reported in the past few years. Equally important is the operating conditions, such as temperature, KOH concentration, and testing/cell running time. The operation temperature in a Zn–air battery is low (typically room temperature). This could be taken as positive news for the stability of the membrane, considering the drastic increase in degradation rate with temperature. Membranes regarded as unstable, such as benzyl-quaternized PPO-based AEMs, have been recently reported to be stable in 7 M KOH solution (30 °C) for 150 h [66]. The prospects for alkaline AEMs in low-temperature fuel cells have been reviewed elsewhere [102].

On the other hand, not so many options are available when it comes to the polymer backbone. Compared to cation groups, less attention has been given to the polymer backbones. This could be due to their relative stability compared to the cations. However, when considering the long term stability of AEMs, they should also be taken into account. To date, different polymer backbones including poly (phenylene) [89], PPO [92,103,104], polybenzimidazole [105], and poly (ether sulfone) [106] have been used to prepare AEMs. For instance, PPO, an electron-rich aromatic backbone, has often been used because of its high glass transition temperature (215 °C), excellent mechanical strength, good alkaline stability, and commercial availability [107]. The polymer, before the introduction of cations, has been proven to be stable (via spectroscopy and tensile tests) in 1 and 6 M KOH at 60 °C. On the other hand, however, when functionalized with QAs, it has been reported to degrade under the same testing [107] and aggressive conditions [108] (high temperature (above 80 °C) and high pH (1–4 M NaOH)), and under oxidative conditions [109].

Various degradation routes have been identified for different polymer backbones. Figure 10 shows the degradation mechanisms of polyvinylidene fluoride (PVDF)-, polysulfone-, polystyrene-, and aryl-ether-containing polymers. Attack by OH<sup>−</sup> ions is believed to be the main reason for polymer backbone degradation. For instance, PVDF is susceptible to dehydrofluorination, which is attributed to the attack of OH<sup>−</sup>, resulting in an E2 elimination, as shown in Figure 10a [110–112]. Similarly, polysulfone-based AEMs are known to be susceptible to both ether hydrolysis and quaternary carbon hydrolysis due to OH<sup>−</sup> attack [108,113] (Figure 10b). Moreover, oxygen [114] and other byproducts, such as products formed by hydroxylation reaction and carbonyl function [115], can further degrade the polymer backbone. For example, the formation of carboxylic acid as a result of the oxidation of a polystyrene backbone can occur [116] (Figure 10d,c). Figure 10d shows aryl ether cleavage of a quaternized aryl-ether-containing polymer backbone.



**Figure 10.** Polymer backbone degradation pathways for PVDF (a) [117], polysulfone (b) [118], polystyrene (c) [116], and aryl-ether containing (d) [119] polymers.

On the other hand, polymers without aryl ether bonds (e.g., poly (biphenyl alkylene)s) remain stable when treated with KOH solution [120] (Figure 11). Quaternized aryl-ether-free polyaromatics are believed to be promising AEM materials due to their outstanding alkaline stability. Similar high alkaline stability is expected to be achieved by using carbon–carbon polymer-backbones free of ether linkages [121]. The stability and performance of AEMs employing state-of-the-art aryl-ether-free polyaromatics in comparison with those employing polyolefins and aryl-ether-containing polyaromatics have been reviewed elsewhere [122].

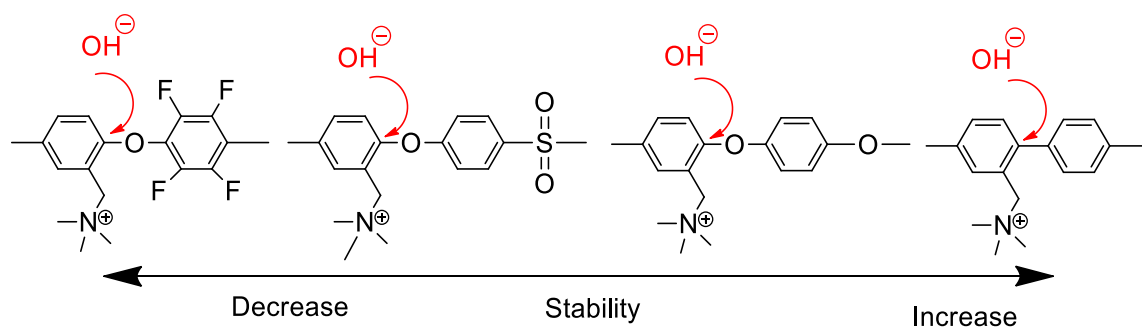


**Figure 11.** Comparison of various polyaromatic polymer backbone stability [119,122–124].

Therefore, it is necessary to combine the three strategies (use of a stable cation, selection of a stable polymer backbone, and good phase separation between the two domains) in order to prepare an AEM with high alkaline stability. For instance, AEMs prepared using poly (phenylene) or carbon–carbon bonded polymers as polymer backbone and N-spirocyclic QA or substituted imidazolium cations could provide an acceptable alkaline stability, especially at low temperatures. Such membranes are expected to have better alkaline stability than the BTMA-based reference membranes. Figure 12 presents the three strategies used (selection of polymer backbone and cation and phase separation) to develop alkaline stable AEMs.

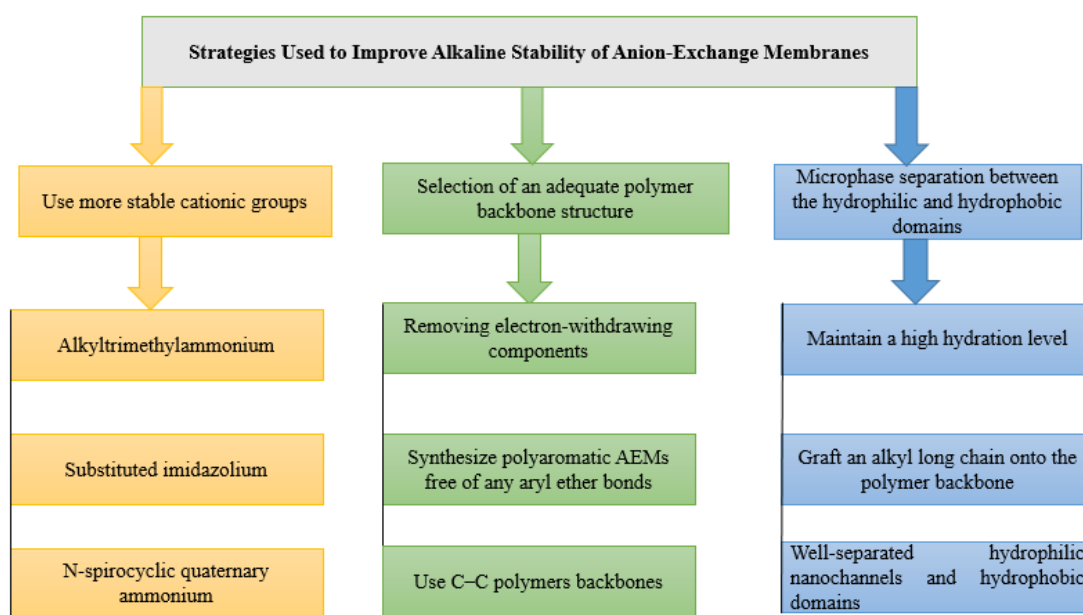


Figure 12. Strategies used to prepare alkaline stable AEMs.

### 3.2. Hydroxide Conductivity

Hydroxide ionic conductivity is another vital parameter for AEMs when employed in electrochemical devices, as hydroxide ions are the main charge carrier. AEMs with adequate anion conductivity are required for high-performance batteries. For this reason, there have been a lot of efforts and improvements reported in the literature [87,116]. Proton conductivity of proton exchange membranes (PEM) has been used as a reference for the values the hydroxide conductivity of AEMs should be reaching, even though the two systems involve different membranes (with different chemical natures and structure), and different transporting species, electrolyte, and operating conditions. Generally speaking, the hydroxide conductivity of AEMs is much lower versus that of the proton conductivity in PEMs for three widely accepted reasons [87]: (i) the lower specific conductivity of  $\text{OH}^-$  ions in a diluted aqueous solution compared to protons (2 times lower), (ii) possible partial carbonation during  $\text{OH}^-$  conductivity measurement (specific conductivity of the  $\text{CO}_3^{2-}$  is 4 times lower than that of  $\text{OH}^-$ ), and (iii) the requirement of a higher water content to form the sub-phase of solvated ions that enables ionic percolation in case of poly-hydrocarbon-based AEMs than that which is required in the case of perfluorinated PEMs.

In order to significantly increase  $\text{OH}^-$  ion conductivity of AEMs, it is important to understand the transport mechanisms of  $\text{OH}^-$  ions and the factors affecting it. Similar to proton conductivity, it has been experimentally observed that  $\text{OH}^-$  conductivity depends on environmental conditions such as temperature, water content associated with the relative humidity, and membrane morphology [125–127]. For this reason, hydroxide transport mechanisms in the AEM are believed to be analogous to the transport of protons in PEMs [128]. Figure 13 presents the possible dominant transport mechanisms for  $\text{OH}^-$  ions in AEMs. The Grotthuss and vehicle mechanisms are considered to be the main

transport mechanisms [129]. Therefore, the concentration of fixed charges, interconnectivity of the hydrophilic ionic nanochannels, and the water content of membranes control the  $\text{OH}^-$  transport in the membrane phase.

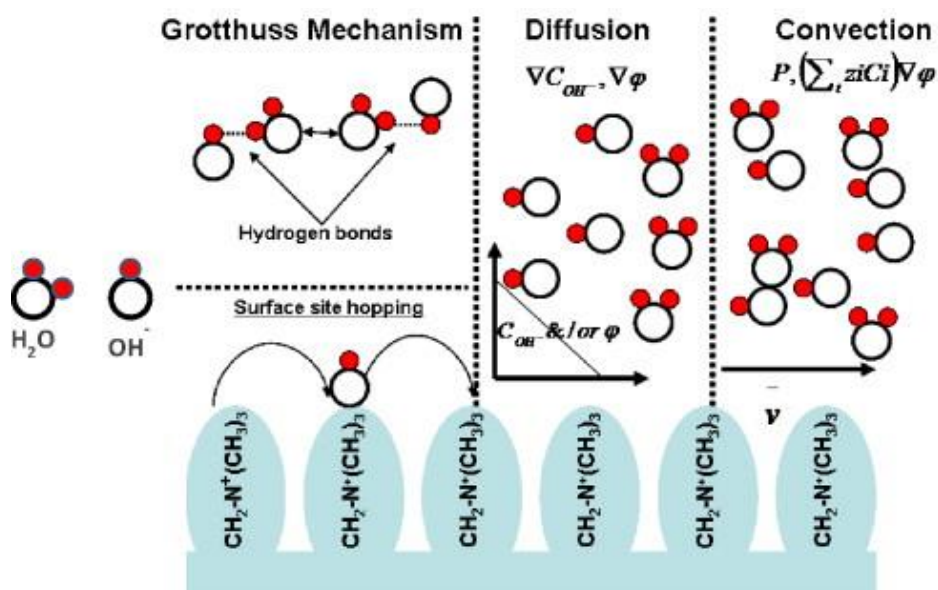


**Figure 13.** Dominant transport mechanisms for hydroxide ions in AEMs. Reproduced with permission from Reference [128]. Copyright 2010, The Electrochemical Society.

However, with the increase in hydroxide conductivity of AEMs, selectivity and mechanical properties usually become the new two challenges. This is due to the high water uptake, which induces the swelling of the membrane. First, the mechanical integrity of the membrane could be in danger with too much water uptake and swelling. Second, with high water uptake, zincate ions in Zn–air batteries could cross from the Zn anode to the air cathode. On the other hand, as discussed in Section 2, the low cyclic stability of the A201<sup>®</sup> membrane was found to be due to the low water uptake of the membrane. Therefore, optimized water uptake, not excessively high, and not affecting the mechanical integrity and the selectivity of the membranes should be achieved.

Various strategies have been employed to enhance the hydroxide conductivity of AEMs. One strategy is to prepare AEMs with well-developed phase separation between the hydrophilic and hydrophobic domains, as discussed in Section 3.1. Large and well-organized nanochannels would allow the transportation of hydroxide ions in a faster way. The second method is to prepare polymer electrolyte AEMs, which usually have high hydroxide ion conductivity due to their hydrophilic nature. A highly conductive (123 mS/cm at room temperature in water), AEM composed of poly (vinyl alcohol)/guar hydroxypropyltrimonium chloride (PGG-GP) retaining high swelling resistance was developed by using glutaraldehyde (GA) and pyrrole-2-carboxaldehyde as binary cross-linkers [130] (Figure 14). Two reasons were identified for this high conductivity as a result of the binary cross-linking process: (i) the highly electronegative nitrogen atoms increased the density of the electron clouds on their neighboring carbon atoms, which made the heterocyclic ring more active, thereby facilitating the chain segment motion and the ionic transport, and (ii) a microphase-separated structure and larger hydrophilic ionic clusters were constructed, forming ion transport pathways. The PGG-GP polymer electrolyte-based, flexible, all-solid-state Zn–air batteries displayed a peak power density of 50.2 mW/cm<sup>2</sup> and promising cycling stability (9 h at 2 mA/cm).

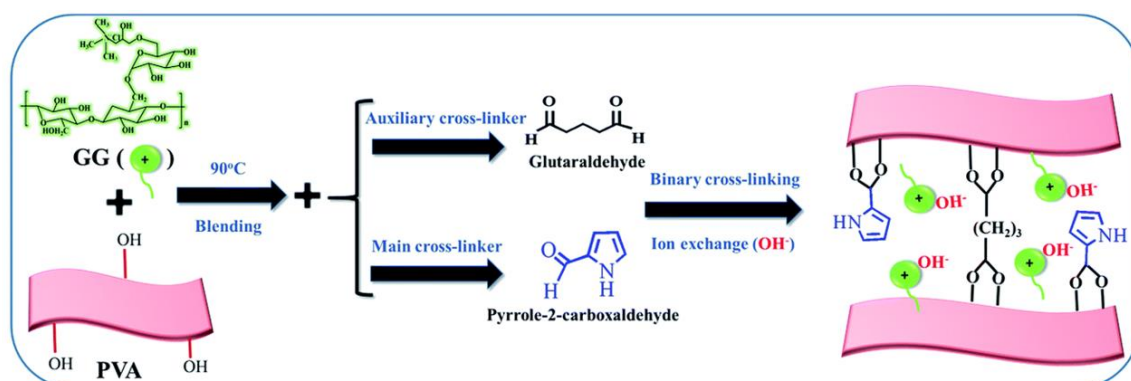


**Figure 14.** Fabrication process of the poly (vinyl alcohol)/guar hydroxypropyltrimonium chloride (PGG-GP) membrane. Reproduced from Reference [130] with permission from The Royal Society of Chemistry.

### 3.3. Lack of Suitable High-Performing AEMs Designed for Alkali Metal–Air Flow Batteries

A suitable AEM which fits all requirements is yet to be developed. AEMs designed for other applications may not be applicable for long-term use in alkali metal–air batteries. To achieve the full potential of these batteries, they must be complemented with a suitable high-performing AEM, which is still not commercially available [73]. There are some commercially available AEMs, such as Tokuyama (A201<sup>®</sup>) and Fumatech (FAA<sup>®</sup>-3). However, not only were these membranes not primarily designed for flow batteries, but are also very little studies regarding the compatibility of these membranes in alkali metal–air flow batteries. For instance, the A201<sup>®</sup> membrane’s relatively high anisotropic swelling and low water uptake were found to critically lower the performances, life, and cyclability of secondary Zn–air batteries. All in all, full scale testing these membranes in an optimized system is needed to fully understand their performance and weaknesses.

Another important issue often neglected is that AEMs prepared for alkaline Zn–air flow batteries should selectively permeate OH<sup>−</sup> ions while blocking the passage of larger size zincate ions from the Zn electrode to the air one. Both the zincate and OH<sup>−</sup> ions have the same charge and can move through the membrane. Therefore, synthesizing AEMs with an optimized ionic nanochannel size is needed. Moreover, the water uptake capacity of these membranes needs to be investigated and optimized for the same purpose.

### 3.4. Lack of Standardization in Membrane Testing Protocol

Standardized testing methodologies are required for the key properties of AEMs, especially alkaline stability, OH<sup>−</sup> conductivity, mechanical properties, and device performance and durability [121]. As established in Section 2, the anisotropic swelling degree, OH<sup>−</sup> conductivity, and water uptake have been reported to be critical for the performance and cyclability of the AEMs used in rechargeable Zn–air batteries. To understand the need for standardized testing methods, we have collected the anisotropic swelling degree and water uptake of the commercial A201<sup>®</sup> membrane as reported in four different publications (Table 2). As shown in Table 2, for the same commercial membranes, different values have been reported. One can imagine how difficult it could be to compare different self-prepared membranes across different studies. Therefore, for comparison purposes and to advance the preparation of robust and high-performing AEMs for alkali metal–air batteries, it is important to establish common standardized testing and characterizing protocols.

**Table 2.** Anisotropic swelling degree of the A201<sup>®</sup> membrane reported in the literature.

Membrane	Anisotropic Swelling Degree	Water Uptake (g/g) (Room Temperature)	Ref.
A201 <sup>®</sup>	3	0.25	[70]
	3.8	0.41	[61]
	3.9	0.44	[131]
	4.4	0.443	[69]

Another important parameter of AEMs which has been widely reported to affect the cell performance and lifespan are their stability and hydroxide conductivity. For instance, the long-term alkaline stability of AEMs is a major concern when intended for long-term use under highly alkaline solution and high temperature. However, one thing worth mentioning is the difficulty, if not impossibility, of comparing the alkaline stability of membranes with those reported in the literature, since there is no standardized testing protocol, such as immersion/testing time, KOH concentration, or temperature and characterizing methods.

One good start was the establishment of a practical thermogravimetric method for quantifying IEC decrease of hydroxide exchange membranes during intrinsic degradation by hydroxide ions. The basis of this method was that the degradation occurred under controlled temperatures and relative humidity conditions while the sample weight (associated with water uptake) was continuously reported. As a result, the degradation rate was reported to be dependent on temperature, relative humidity, and total water content [131].

Similarly, a comparison of reported data for OH<sup>-</sup> conductivity of different AEMs has been almost impossible due to the quick exchange with larger and less mobile anions (CO<sub>3</sub><sup>2-</sup> and HCO<sub>3</sub><sup>-</sup>) when the membrane is in contact with air. This is believed to be one of the reasons why OH<sup>-</sup> conductivity of AEMs is so low compared to proton conductivity of PEMs. Therefore, hydroxide conductivity is another parameter that needs to be standardized. Three methods have been proposed to avoid carbonation and its negative effects: (i) use of gas-purged water during the exchange process [74] or during measurement [132,133], (ii) use of a glovebox containing an inert gas under CO<sub>2</sub>-free conditions [132], and (iii) forcing the release of the larger (bi)carbonate anions as CO<sub>2</sub> gas by applying an external electric current through the membrane [134].

In the third method, as shown in Figure 15, OH<sup>-</sup> is produced at one electrode during the application of current and HCO<sub>3</sub><sup>-</sup>/CO<sub>3</sub><sup>2-</sup> are purged as CO<sub>2</sub> at the other electrode. In the condition used (a large amount of water associated with the humidified ambient gas), after about 30 h of applying 100 μA, all the HCO<sub>3</sub><sup>-</sup>/CO<sub>3</sub><sup>2-</sup> is removed from the membrane and the OH<sup>-</sup> ion conductivity becomes stable with time. The resistance of the membrane was measured using a standard four probe method, followed by measurement of in-plane conductivity. The method is reliable and reproducible. Moreover, it does not require the use of glovebox or expensive fuel cell tests, and neither does it involve chemical steps to convert the membrane into its hydroxide form. However, the time duration for measuring a single membrane sample seems long compared to the other more conventional methods. The OH<sup>-</sup> ion conductivity measurement process is represented schematically in Figure 15.

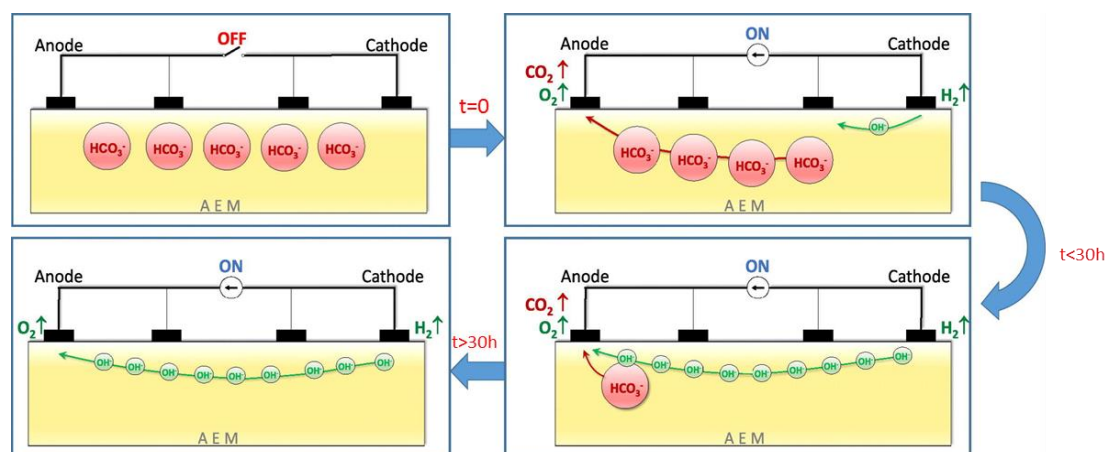


**Figure 15.** Schematic illustration of the processes taking place in the AEM while applying direct current under the conditions of  $\text{OH}^-$  conductivity test. Adapted with permission from Reference [134]. Copyright Elsevier 2018.

### 3.5. Cost

Another important parameter when preparing AEMs is their price. The price of the membrane affects the overall price of the battery and the possibility of their mass production. Lowering membrane costs will help reduce the overall price of the batteries, thereby increasing their widespread use.

After all, one of the major advantages of AEM-based electrochemical systems is their potential to eliminate the use of platinum as a catalyst, which is costly and limited in abundance. A highly conductive and stable AEM that is expensive may not be readily applicable. Therefore, the membranes need to be produced at an acceptable or affordable price. For instance, the FAA<sup>®</sup>-3-50 membrane is currently sold at a price of \$17.00 for a 10 cm × 10 cm membrane [74].

Therefore, development and production of cost-effective membranes with high durability and performance is needed. This can be achieved by using low-cost polymers such as polyvinyl alcohol and chitosan as polymer backbones. The synthesis method used also greatly affects the final cost of membranes. Equally important is the price of the cations used. This is a topic which requires cooperation between academia and industry.

## 4. Summary and Outlooks

In summary, this paper briefly reviewed the recent advances of AEMs for alkali metal–air batteries. Metal–air flow batteries have the potential to become the energy storage of choice in the future because of their low cost, environmental friendliness, and huge energy storage capacity. As a result, in recent years, they have been given intense research and development. To achieve their goal, an excellent cathode, anode, and electrolyte are required in addition to suitable, excellent, and low-cost membrane.

One of the many challenges preventing these batteries (typically, rechargeable Zn–air batteries) from reaching their full potential as the next generation of electrochemical energy storage is the lack of suitable membrane separators. Despite their critical importance, the preparation and development of suitable membranes have been given only a little attention. Various membranes, including porous membranes and modified porous membrane separators, have been tested as separators. Usually, porous membrane separators taken from Li-based batteries are used. Despite their superior mechanical strength and broad electrochemical stability window, they are not able to block the crossover of zincate ions due to their too large pores, thus leading to increased cell polarization and decreased long-term durability of the batteries. To solve this problem, composite and cation-exchange membranes have been tested; however, their  $\text{OH}^-$  conductivities have been reported to be low.

The use of AEMs could address this problem by selectively limiting the crossover of unwanted ions. Despite these high recommendations, there have been few papers published studying the performance

of alkaline AEMs in alkali metal–air batteries. In this review paper, correlations between the properties of the AEMs (such as conductivity, water uptake, and swelling ratio) and battery performances (such as capacity and cyclic performance stability) were established. This review mainly discussed the use of AEMs in Zn–air batteries. However, similar results and challenges should be expected in other batteries as well.

Among the commercial membranes, the A201<sup>®</sup> membrane has been relatively tested to a certain extent. Since the membranes were not initially designed and tuned for this specific application, the performance and durability of A201<sup>®</sup>-based batteries are limited. The A201<sup>®</sup> membrane's high anisotropic swelling ratio and relatively low uptake have been critically found to be the main reasons. On the other hand, AEMs specifically designed for these applications have been shown to be promising. Based on the collected results of membrane properties and battery performances, AEMs with small anisotropic swelling and high water uptake are required for superior performance of batteries. An AEM with structural stability via decrease of swelling in both the through-plane and in-plane directions is needed for long-term battery cycling operation. Testing other commercially available AEMs in alkali metal–air batteries is also needed.

To fully implement these membranes, there are some challenges that need to be overcome first. The main problem associated with the use of AEMs is their limited alkaline stability. Different strategies have been proposed and employed to improve and solve this problem. The major degradation mechanisms, especially for the commonly used cations and polymer backbones, are discussed in this review. Moreover, a perspective on how to avoid these degradations is outlined. For example, quaternized, aryl-ether-free polyaromatics are promising AEM materials because of their outstanding alkaline stability. In general, polymers that are free of electron-withdrawing groups in their backbone such as poly(phenylene) and carbon–carbon bonded polymers have shown promising results and are expected to provide the required level of stability. On the other hand, the stability of cations at harsh and high temperatures is a hot research topic at the moment. AEMs incorporating relatively stable cations and unique aromatic polymers free of electron-withdrawing groups in the backbone have been reported with promising results. Additionally, the morphology of AEMs has been reported to play a vital role in determining the rate of chemical degradation. Therefore, more efforts are needed to develop more stable membranes by employing these strategies in combination.

The degradation of membranes by OH<sup>−</sup> is known to speed up with increasing temperature. However, unlike most AEM fuel cells, the operating temperature of alkaline metal–air batteries is room temperature. This low-temperature operation plays an important role in increasing the lifespan of the membrane. AEMs normally regarded to be less stable (tests performed at 80 °C) have shown good alkaline and electrochemical stability in Zn–air batteries when tested at room temperature.

Another possible problem associated with the use of AEMs in alkali metal–air batteries application is their low ion conductivity at low temperatures. The low conductivity of these membranes is due to the large size of hydroxide ions (compared to protons) and to the carbonation process. There has been a lot of improvement in this regard as well. AEMs that are highly conductive have been reported in the literature. However, with an increase in water uptake and hydroxide conductivity, care must be taken not to affect the integrity and selectivity of the membranes. Therefore, an adequate conductive membrane with unaffected mechanical/structural integrity and selectivity is required.

Another vital property of AEMs, which should be given huge attention, is the size of their ionic nanochannels, and their conductivity and orientation, in order to decrease the membrane tortuosity and increase the through-plane membrane conductivity. The size of the nanochannels determines the selectivity of the membrane. Therefore, attention should be given to membrane synthesis in order to form channels with an optimal size, which would allow the passage of hydroxide ions and block other species such as zincate ions.

Moreover, the lack of standardizing testing protocols is another challenge. For instance, the water uptake and anisotropic swelling ratio even of a commercial A201<sup>®</sup> membrane has been found to be different in different studies, indicating the need for a standardized testing protocol.

**Funding:** This project has received funding from the European Union’s Horizon 2020 research and innovation programme under the Marie Skłodowska-Curie Grant Agreement no. 765289.

**Conflicts of Interest:** The authors declare no conflict of interest.

## References

1. Wei, X.; Pan, W.; Duan, W.; Hollas, A.; Yang, Z.; Li, B.; Nie, Z.; Liu, J.; Reed, D.; Wang, W.; et al. Materials and systems for organic redox flow batteries: Status and challenges. *ACS Energy Lett.* **2017**, *2*, 2187–2204. [[CrossRef](#)]
2. U.S. Energy Information Administration (EIA). International Energy Outlook 2016 with Projections to 2040. 2016. Available online: [https://www.eia.gov/outlooks/ieo/pdf/0484\(2016\).pdf](https://www.eia.gov/outlooks/ieo/pdf/0484(2016).pdf) (accessed on 10 June 2019).
3. Chang, Z.; Zhang, X. Introduction to metal-air batteries: Theory and basic principles. *Met.-Air Batter.* **2018**, 1–9. [[CrossRef](#)]
4. Janoschka, T.; Martin, N.; Hager, M.D.; Schubert, U.S. An aqueous redox-flow battery with high capacity and power: The TEMPTMA/MV system. *Angew. Chem. Int. Ed.* **2016**, *55*, 14427–14430. [[CrossRef](#)] [[PubMed](#)]
5. Cheng, F.; Chen, J. Metal-air batteries: From oxygen reduction electrochemistry to cathode catalysts. *Chem. Soc. Rev.* **2012**, *41*, 2172–2192. [[CrossRef](#)] [[PubMed](#)]
6. May, G.J.; Davidson, A.; Monahov, B. Lead batteries for utility energy storage: A review. *J. Energy Storage* **2018**, *15*, 145–157. [[CrossRef](#)]
7. Pinnangudi, B.; Kuykendal, M.; Bhadra, S. Smart grid energy storage. *Power Grid.* **2017**, 93–135. [[CrossRef](#)]
8. Du, P.; Lu, N.; Beaudin, M.; Zareipour, H.; Schellenberg, A.; Rosehart, W. Energy storage for mitigating the variability of renewable electricity. *Sources Energy Storage Smart Grids* **2014**, *14*, 1–33. [[CrossRef](#)]
9. Mauger, A.; Julien, C.M. Critical review on lithium-ion batteries: Are they safe? sustainable? *Ionics* **2017**, *23*, 1933–1947. [[CrossRef](#)]
10. Blomgren, G.E. The development and future of lithium ion batteries. *J. Electrochem. Soc.* **2017**, *164*, A5019–A5025. [[CrossRef](#)]
11. Bruce, P.G.; Freunberger, S.A.; Hardwick, L.J.; Tarascon, J.-M. Li-O<sub>2</sub> and Li-S batteries with high energy storage. *Nat. Mater.* **2012**, *11*, 19–29. [[CrossRef](#)]
12. Feng, X.; Ouyang, M.; Liu, X.; Lu, L.; Xia, Y.; He, X. Thermal runaway mechanism of lithium ion battery for electric vehicles: A review. *Energy Storage Mater.* **2018**, *10*, 246–267. [[CrossRef](#)]
13. Sankarasubramanian, S.; Kahky, J.; Ramani, V. Tuning anion solvation energetics enhances potassium-oxygen battery performance. *Proc. Natl. Acad. Sci. USA* **2019**, *116*, 14899–14904. [[CrossRef](#)] [[PubMed](#)]
14. Zhang, X.; Wang, X.-G.; Xie, Z.; Zhou, Z. Recent progress in rechargeable alkali metal-air batteries. *Green Energy Environ.* **2016**, *1*, 4–17. [[CrossRef](#)]
15. Li, Y.; Lu, J. Metal-air batteries: Will they be the future electrochemical energy storage device of choice? *ACS Energy Lett.* **2017**, *2*, 1370–1377. [[CrossRef](#)]
16. Mainar, A.R.; Iruin, E.; Colmenares, L.C.; Kvasha, A.; de Meatza, I.; Bengoechea, M.; Leonet, O.; Boyano, I.; Zhang, Z.; Blazquez, J.A. An overview of progress in electrolytes for secondary zinc-air batteries and other storage systems based on zinc. *J. Energy Storage* **2018**, *15*, 304–328. [[CrossRef](#)]
17. Mori, R. All solid state rechargeable aluminum-air battery with deep eutectic solvent based electrolyte and suppression of byproducts formation. *RSC Adv.* **2019**, *9*, 22220–22226. [[CrossRef](#)]
18. Wang, C.; Yu, Y.; Niu, J.; Liu, Y.; Bridges, D.; Liu, X.; Pooran, J.; Zhang, Y.; Hu, A. Recent progress of metal-air batteries—A mini review. *Appl. Sci.* **2019**, *9*, 2787. [[CrossRef](#)]
19. McKerracher, R.D.; Poncedeleon, C.; Wills, R.G.A.; Shah, A.A.; Walsh, F.C. A review of the iron-air secondary battery for energy storage. *Chempluschem* **2015**, *80*, 323–335. [[CrossRef](#)]
20. Rahman, M.A.; Wang, X.; Wen, C. High energy density metal-air batteries: A review. *J. Electrochem. Soc.* **2013**, *160*, A1759–A1771. [[CrossRef](#)]
21. Pei, P.; Wang, K.; Ma, Z. Technologies for extending zinc-air battery’s cyclife: A review. *Appl. Energy* **2014**, *128*, 315–324. [[CrossRef](#)]
22. Lee, J.-S.; Kim, S.T.; Cao, R.; Choi, N.-S.; Liu, M.; Lee, K.T.; Cho, J. Metal-Air Batteries with High Energy Density: Li-Air versus Zn-Air. *Adv. Energy Mater.* **2011**, *1*, 34–50. [[CrossRef](#)]
23. Sapkota, P.; Kim, H. Zinc-air fuel cell, a potential candidate for alternative energy. *J. Ind. Eng. Chem.* **2009**, *15*, 445–450. [[CrossRef](#)]

24. Fu, J.; Cano, Z.P.; Park, M.G.; Yu, A.; Fowler, M.; Chen, Z. Electrically rechargeable zinc-Air batteries: Progress, challenges, and perspectives. *Adv. Mater.* **2017**, *29*, 1604685. [[CrossRef](#)] [[PubMed](#)]
25. Li, Y.; Dai, H. Recent advances in zinc-air batteries. *Chem. Soc. Rev.* **2014**, *43*, 5257–5275. [[CrossRef](#)]
26. Vincent, C.A.; Scrosati, B. *Modern Batteries: An Introduction to Electrochemical Power Sources*; Elsevier: Amsterdam, The Netherlands, 1997.
27. Barsukov, V.; Beck, F. (Eds.) *New Promising Electrochemical Systems for Rechargeable Batteries*; Springer: Dordrecht, The Netherlands, 1996. [[CrossRef](#)]
28. Zhang, Z.; Zuo, C.; Liu, Z.; Yu, Y.; Zuo, Y.; Song, Y. All-solid-state Al-air batteries with polymer alkaline gel electrolyte. *J. Power Sources* **2014**, *251*, 470–475. [[CrossRef](#)]
29. Liu, Y.; Sun, Q.; Li, W.; Adair, K.R.; Li, J.; Sun, X. A comprehensive review on recent progress in aluminum-air batteries. *Green Energy Environ.* **2017**, *2*, 246–277. [[CrossRef](#)]
30. Mokhtar, M.; Talib, M.Z.M.; Majlan, E.H.; Tasirin, S.M.; Ramli, W.M.F.W.; Daud, W.R.W.; Sahari, J. Recent developments in materials for aluminum-air batteries: A review. *J. Ind. Eng. Chem.* **2015**, *32*, 1–20. [[CrossRef](#)]
31. Yang, S. Design and analysis of aluminum/air battery system for electric vehicles. *J. Power Sources* **2002**, *112*, 162–173. [[CrossRef](#)]
32. Mori, R. A novel aluminium-air rechargeable battery with Al<sub>2</sub>O<sub>3</sub> as the buffer to suppress byproduct accumulation directly onto an aluminium anode and air cathode. *RSC Adv.* **2014**, *4*, 30346–30351. [[CrossRef](#)]
33. Heise, G.W. Air-Depolarized Primary Battery. 1925. Available online: <https://patents.google.com/patent/US1899615A/en> (accessed on 8 October 2019).
34. Zaromb, S. The use and behavior of aluminum anodes in alkaline primary batteries. *J. Electrochem. Soc.* **1962**, *109*, 1125–1130. [[CrossRef](#)]
35. Öjefors, L.; Carlsson, L. An iron-air vehicle battery. *J. Power Sources* **1978**, *2*, 287–296. [[CrossRef](#)]
36. Home-Eos Energy Storage. Available online: <https://eosenergystorage.com/#welcome> (accessed on 4 October 2019).
37. NantEnergy|Progress in Power. Available online: <https://nantenergy.com/> (accessed on 4 October 2019).
38. Zinc8 Energy Solutions. Available online: <https://zinc8energy.com/> (accessed on 4 October 2019).
39. Powair. Available online: <http://www.powair.eu/> (accessed on 4 October 2019).
40. ZAS-Zinc Air Secondary Innovative Nanotech Based Batteries for Efficient Energy Storage. Available online: <https://www.sintef.no/zas> (accessed on 4 October 2019).
41. FlowCamp-the Redox Flow Battery Campus. Available online: <https://www.flowcamp-project.eu/> (accessed on 4 October 2019).
42. Sun, Y.; Liu, X.; Jiang, Y.; Li, J.; Ding, J.; Hu, W.; Zhong, C. Recent advances and challenges in divalent and multivalent metal electrodes for metal-air batteries. *J. Mater. Chem. A* **2019**, *7*, 18183–18208. [[CrossRef](#)]
43. Gu, P.; Zheng, M.; Zhao, Q.; Xiao, X.; Xue, H.; Pang, H. Rechargeable zinc-air batteries: A promising way to green energy. *J. Mater. Chem. A* **2017**, *5*, 7651–7666. [[CrossRef](#)]
44. Blurton, K.F.; Sammells, A.F. Metal/air batteries: Their status and potential—A review. *J. Power Sources* **1979**, *4*, 263–279. [[CrossRef](#)]
45. Liu, P. A Low-Cost Ion Exchange Membrane Separator for Rechargeable Aqueous Batteries. 2018. Available online: <https://ecs.confex.com/ecs/aimes2018/webprogram/Paper115710.html> (accessed on 4 October 2019).
46. Saputra, H.; Othman, R.; Sutjipto, A.G.E.; Muhida, R. MCM-41 as a new separator material for electrochemical cell: Application in zinc-air system. *J. Membr. Sci.* **2011**, *367*, 152–157. [[CrossRef](#)]
47. Kiros, Y. Separation and permeability of zincate ions through membranes. *J. Power Sources* **1996**, *62*, 117–119. [[CrossRef](#)]
48. Kim, H.W.; Lim, J.M.; Lee, H.J.; Eom, S.W.; Hong, Y.T.; Lee, S.Y. Artificially engineered, bicontinuous anion-conducting/-repelling polymeric phases as a selective ion transport channel for rechargeable zinc-air battery separator membranes. *J. Mater. Chem. A* **2016**, *4*, 3711–3720. [[CrossRef](#)]
49. Dewi, E.L.; Oyaizu, K.; Nishide, H.; Tsuchida, E. Cationic polysulfonium membrane as separator in zinc-air cell. *J. Power Sources* **2003**, *115*, 149–152. [[CrossRef](#)]
50. Hwang, H.J.; Chi, W.S.; Kwon, O.; Lee, J.G.; Kim, J.H.; Shul, Y.-G. Selective ion transporting polymerized ionic liquid membrane separator for enhancing cycle stability and durability in secondary zinc-air battery systems. *ACS Appl. Mater. Interfaces* **2016**, *8*, 26298–26308. [[CrossRef](#)]
51. Zinc-Air Secondary Battery. 2014. Available online: <https://patents.google.com/patent/US20140227616> (accessed on 4 October 2019).

52. Metal-Air Battery with Ion Exchange Materials. 2010. Available online: <https://patents.google.com/patent/US20110027666A1/en> (accessed on 4 October 2019).
53. Rechargeable Zinc-Air Flow Battery. 2014. Available online: <https://patents.google.com/patent/WO2015004069A1/en> (accessed on 4 October 2019).
54. Sum, E.; Skyllas-Kazacos, M. A study of the V(II)/V(III) redox couple for redox flow cell applications. *J. Power Sources* **1985**, *15*, 179–190. [[CrossRef](#)]
55. Sum, E.; Rychcik, M.; Skyllas-kazacos, M. Investigation of the V(V)/V(IV) system for use in the positive half-cell of a redox battery. *J. Power Sources* **1985**, *16*, 85–95. [[CrossRef](#)]
56. Skyllas-Kazacos, M.; Grossmith, F. Efficient vanadium redox flow cell. *J. Electrochem. Soc.* **1987**, *134*, 2950–2953. [[CrossRef](#)]
57. Mai, Z.; Zhang, H.; Li, X.; Xiao, S.; Zhang, H. Nafion/polyvinylidene fluoride blend membranes with improved ion selectivity for vanadium redox flow battery application. *J. Power Sources* **2011**, *196*, 5737–5741. [[CrossRef](#)]
58. Zeng, J.; Jiang, C.; Wang, Y.; Chen, J.; Zhu, S.; Zhao, B.; Wang, R. Studies on polypyrrole modified nafion membrane for vanadium redox flow battery. *Electrochem. Commun.* **2008**, *10*, 372–375. [[CrossRef](#)]
59. Xi, J.; Wu, Z.; Qiu, X.; Chen, L. Nafion/SiO<sub>2</sub> hybrid membrane for vanadium redox flow battery. *J. Power Sources* **2007**, *166*, 531–536. [[CrossRef](#)]
60. Wei, Y.; Wang, M.; Xu, N.; Peng, L.; Mao, J.; Gong, Q.; Qiao, J. Alkaline exchange polymer membrane electrolyte for high performance of all-solid-state electrochemical devices. *ACS Appl. Mater. Interfaces* **2018**, *10*, 29593–29598. [[CrossRef](#)]
61. Fumatech GmbH. Available online: <https://www.fumatech.com/Startseite/index.html> (accessed on 5 October 2019).
62. Carmo, M.; Doubek, G.; Sekol, R.C.; Linardi, M.; Taylor, A.D. Development and electrochemical studies of membrane electrode assemblies for polymer electrolyte alkaline fuel cells using FAA membrane and ionomer. *J. Power Sources* **2013**, *230*, 169–175. [[CrossRef](#)]
63. Dekel, D.; Schuster, M.; Ash, U.; Jaouen, F. Critical Raw Materials Elimination by a Top-Down Approach to Hydrogen and Electricity Generation. 2017, pp. 1–13. Available online: <https://cordis.europa.eu/project/rcn/206995/factsheet/en> (accessed on 9 December 2019).
64. Yanagi, H.; Fukuta, K. Anion exchange membrane and ionomer for alkaline membrane fuel cells (AMFCs). *ECS Trans.* **2008**, 257–262. [[CrossRef](#)]
65. Abuin, G.C.; Franceschini, E.A.; Nonjola, P.; Mathe, M.K.; Modibedi, M.; Corti, H.R. A high selectivity quaternized polysulfone membrane for alkaline direct methanol fuel cells. *J. Power Sources* **2015**, *279*, 450–459. [[CrossRef](#)]
66. Abbasi, A.; Hosseini, S.; Somwangthanoj, A.; Mohamad, A.A.; Kheawhom, S. Poly(2,6-Dimethyl-1,4-Phenylene Oxide)-based hydroxide exchange separator membranes for zinc-air battery. *Int. J. Mol. Sci.* **2019**, *20*, 3678. [[CrossRef](#)]
67. Willdorf-Cohen, S.; Mondal, A.; Dekel, D.; Diesendruck, C. Chemical stability of poly(phenylene oxide)-based ionomers in an anion exchange-membrane fuel cell environment. *J. Mater. Chem. A* **2018**. [[CrossRef](#)]
68. Fu, J.; Zhang, J.; Song, X.; Zarrin, H.; Tian, X.; Qiao, J.; Rasen, L.; Li, K.; Chen, Z. A flexible solid-state electrolyte for wide-scale integration of rechargeable zinc-air batteries. *Energy Environ. Sci.* **2016**, *9*, 663–670. [[CrossRef](#)]
69. Zhang, J.; Fu, J.; Song, X.; Jiang, G.; Zarrin, H.; Xu, P.; Li, K.; Yu, A.; Chen, Z. Laminated cross-linked nanocellulose/graphene oxide electrolyte for flexible rechargeable zinc-air batteries. *Adv. Energy Mater.* **2016**, *6*, 1600476. [[CrossRef](#)]
70. Zarrin, H.; Sy, S.; Fu, J.; Jiang, G.; Kang, K.; Jun, Y.-S.; Yu, A.; Fowler, M.; Chen, Z. Molecular functionalization of graphene oxide for next-generation wearable electronics. *ACS Appl. Mater. Interfaces* **2016**, *8*, 25428–25437. [[CrossRef](#)] [[PubMed](#)]
71. Fumasep® Membrane Types Redox-Flow-Batteries. Available online: <https://www.fumatech.com> (accessed on 5 October 2019).
72. Kwon, O.; Hwang, H.J.; Ji, Y.; Jeon, O.S.; Kim, J.P.; Lee, C.; Shul, Y.G. Transparent bendable secondary zinc-air batteries by controlled void ionic separators. *Sci. Rep.* **2019**, *9*, 3175. [[CrossRef](#)] [[PubMed](#)]

73. Soni, R.; Bhang, S.N.; Kurungot, S. A 3-D nanoribbon-like Pt-free oxygen reduction reaction electrocatalyst derived from waste leather for anion exchange membrane fuel cells and zinc-air batteries. *Nanoscale* **2019**, *11*, 7893–7902. [CrossRef]
74. Technical Datasheet-Fumapem® FAA-3-50. Available online: <https://fuelcellstore.com/spec-sheets/fumapem-faa-3-50-technical-specifications.pdf> (accessed on 8 October 2019).
75. Mandal, M.; Huang, G.; Kohl, P.A. Highly conductive anion-exchange membranes based on cross-linked poly(norbornene): Vinyl addition polymerization. *ACS Appl. Energy Mater.* **2019**, *2*, 2447–2457. [CrossRef]
76. Wang, L.; Bellini, M.; Miller, H.A.; Varcoe, J.R. A high conductivity ultrathin anion-exchange membrane with 500+ h alkali stability for use in alkaline membrane fuel cells that can achieve 2 W cm<sup>-2</sup> at 80 °C. *J. Mater. Chem. A* **2018**, *6*, 15404–15412. [CrossRef]
77. Fu, J.; Qiao, J.; Lv, H.; Ma, J.; Yuan, X.-Z.; Wang, H. Alkali doped poly(vinyl alcohol) (PVA) for anion-exchange membrane fuel cells: Ionic conductivity, chemical stability and FT-IR characterizations. *ECS Trans.* **2010**, *25*, 15–23. [CrossRef]
78. Yokota, N.; Shimada, M.; Ono, H.; Akiyama, R.; Nishino, E.; Asazawa, K.; Miyake, J.; Watanabe, M.; Miyatake, K. Aromatic copolymers containing ammonium-functionalized oligophenylene moieties as highly anion conductive membranes. *Macromolecules* **2014**, *47*, 8238–8246. [CrossRef]
79. Sun, L.; Guo, J.; Zhou, J.; Xu, Q.; Chu, D.; Chen, R. Novel nanostructured high-performance anion exchange ionomers for anion exchange membrane fuel cells. *J. Power Sources* **2012**, *202*, 70–77. [CrossRef]
80. Zhang, S.; Li, C.; Xie, X.; Zhang, F. Novel cross-linked anion exchange membranes with diamines as ionic exchange functional groups and crosslinking groups. *Int. J. Hydrogen Energy* **2014**, *39*, 13718–13724. [CrossRef]
81. Ran, J.; Wu, L.; Varcoe, J.R.; Ong, A.L.; Poynton, S.D.; Xu, T. Development of imidazolium-type alkaline anion exchange membranes for fuel cell application. *J. Membr. Sci.* **2012**, *415–416*, 242–249. [CrossRef]
82. Yoshimura, K.; Koshikawa, H.; Yamaki, T.; Shishitani, H.; Yamamoto, K.; Yamaguchi, S.; Tanaka, H.; Maekawa, Y. Imidazolium cation based anion-conducting electrolyte membranes prepared by radiation induced grafting for direct hydrazine hydrate fuel cells. *J. Electrochem. Soc.* **2014**, *161*, F889–F893. [CrossRef]
83. Cotanda, P.; Sudre, G.; Modestino, M.A.; Chen, X.C.; Balsara, N.P. High anion conductivity and low water uptake of phosphonium containing diblock copolymer membranes. *Macromolecules* **2014**, *47*, 7540–7547. [CrossRef]
84. Noonan, K.J.T.; Hugar, K.M.; Kostalik, H.A.; Lobkovsky, E.B.; Abruña, H.D.; Coates, G.W. Phosphonium-functionalized polyethylene: A new class of base-stable alkaline anion exchange membranes. *J. Am. Chem. Soc.* **2012**, *134*, 18161–18164. [CrossRef]
85. Sajjad, S.D.; Hong, Y.; Liu, F. Synthesis of guanidinium-based anion exchange membranes and their stability assessment. *Polym. Adv. Technol.* **2014**, *25*, 108–116. [CrossRef]
86. Li, W.; Wang, S.; Zhang, X.; Wang, W.; Xie, X.; Pei, P. Degradation of guanidinium-functionalized anion exchange membrane during alkaline environment. *Int. J. Hydrogen Energy* **2014**, *39*, 13710–13717. [CrossRef]
87. Gottesfeld, S.; Dekel, D.R.; Page, M.; Bae, C.; Yan, Y.; Zelenay, P.; Kim, Y.S. Anion exchange membrane fuel cells: Current status and remaining challenges. *J. Power Sources* **2018**, *375*, 170–184. [CrossRef]
88. Couture, G.; Ladmiral, V.; Améduri, B. Comparison of epoxy- and cyclocarbonate-functionalised vinyl ethers in radical copolymerisation with chlorotrifluoroethylene. *J. Fluor. Chem.* **2015**, *171*, 124–132. [CrossRef]
89. Hibbs, M.R. Alkaline stability of poly(phenylene)-based anion exchange membranes with various cations. *J. Polym. Sci. Part B Polym. Phys.* **2013**, *51*, 1736–1742. [CrossRef]
90. Jannasch, P. Tethering cations to aromatic polymers via flexible spacers to enhance the performance of alkaline fuel cell membranes. *ECS Trans.* **2015**, *69*, 369–375. [CrossRef]
91. Marino, M.G.; Kreuer, K.D. Alkaline stability of quaternary ammonium cations for alkaline fuel cell membranes and ionic liquids. *ChemSusChem* **2015**, *8*, 513–523. [CrossRef] [PubMed]
92. Li, N.; Yan, T.; Li, Z.; Thurn-Albrecht, T.; Binder, W.H. Comb-shaped polymers to enhance hydroxide transport in anion exchange membranes. *Energy Environ. Sci.* **2012**, *5*, 7888–7892. [CrossRef]
93. Shin, D.W.; Guiver, M.D.; Lee, Y.M. Hydrocarbon-based polymer electrolyte membranes: Importance of morphology on ion transport and membrane stability. *Chem. Rev.* **2017**, *117*, 4759–4805. [CrossRef]
94. Dekel, D.R.; Willdorf, S.; Ash, U.; Amar, M.; Pusara, S.; Dhara, S.; Srebnik, S.; Diesendruck, C.E. The critical relation between chemical stability of cations and water in anion exchange membrane fuel cells environment. *J. Power Sources* **2018**, *375*, 351–360. [CrossRef]

95. Dekel, D.R.; Amar, M.; Willdorf, S.; Kosa, M.; Dhara, S.; Diesendruck, C.E. Effect of water on the stability of quaternary ammonium groups for anion exchange membrane fuel cell applications. *Chem. Mater.* **2017**, *29*, 4425–4431. [[CrossRef](#)]
96. Strasser, D.J.; Graziano, B.J.; Knauss, D.M. Base stable poly(diallylpiperidinium hydroxide) multiblock copolymers for anion exchange membranes. *J. Mater. Chem. A* **2017**, *5*, 9627–9640. [[CrossRef](#)]
97. Olsson, J.S.; Pham, T.H.; Jannasch, P. Poly(*N,N*-diallylazacycloalkane)s for anion-exchange membranes functionalized with *N*-spirocyclic quaternary ammonium cations. *Macromolecules* **2017**, *50*, 2784–2793. [[CrossRef](#)]
98. Pham, T.H.; Jannasch, P. Aromatic polymers incorporating bis-*N*-spirocyclic quaternary ammonium moieties for anion-exchange membranes. *ACS Macro Lett.* **2015**, *4*, 1370–1375. [[CrossRef](#)]
99. Vogel, C.; Komber, H.; Meier-Haack, J. Temperature-stable anion-exchange materials from cyclopolymerization of quaternary ammonium halides. *React. Funct. Polym.* **2017**, *117*, 34–42. [[CrossRef](#)]
100. Thomas, O.D.; Soo, K.J.W.Y.; Peckham, T.J.; Kulkarni, M.P.; Holdcroft, S. A stable hydroxide-conducting polymer. *J. Am. Chem. Soc.* **2012**, *134*, 10753–10756. [[CrossRef](#)] [[PubMed](#)]
101. Fan, J.; Wright, A.G.; Britton, B.; Weissbach, T.; Skalski, T.J.G.; Ward, J.; Peckham, T.J.; Holdcroft, S. Cationic polyelectrolytes, stable in 10 M KOH aq at 100 °C. *ACS Macro Lett.* **2017**, *6*, 1089–1093. [[CrossRef](#)]
102. Varcoe, J.R.; Slade, R.C.T. Prospects for alkaline anion-exchange membranes in low Ttemperature fuel cells. *Fuel Cells* **2005**, *5*, 187–200. [[CrossRef](#)]
103. Liu, Y.; Zhang, B.; Kinsinger, C.L.; Yang, Y.; Seifert, S.; Yan, Y.; Maupin, C.M.; Liberatore, M.W.; Herring, A.M. Anion exchange membranes composed of a poly(2,6-dimethyl-1,4-phenylene oxide) random copolymer functionalized with a bulky phosphonium cation. *J. Membr. Sci.* **2016**, *506*, 50–59. [[CrossRef](#)]
104. Dang, H.-S.; Jannasch, P. Alkali-stable and highly anion conducting poly(phenylene oxide)s carrying quaternary piperidinium cations. *J. Mater. Chem. A* **2016**, *4*, 11924–11938. [[CrossRef](#)]
105. Lin, J.; Yan, X.; He, G.; Chen, W.; Zhen, D.; Li, T.; Ma, L.; Wu, X. Thermoplastic interpenetrating polymer networks based on polybenzimidazole and poly(1, 2-dimethyl-3-allylimidazolium) for anion exchange membranes. *Electrochim. Acta* **2017**, *257*, 9–19. [[CrossRef](#)]
106. Lin, C.X.; Huang, X.L.; Guo, D.; Zhang, Q.G.; Zhu, A.M.; Ye, M.L.; Liu, Q.L. Side-chain-type anion exchange membranes bearing pendant quaternary ammonium groups via flexible spacers for fuel cells. *J. Mater. Chem. A* **2016**, *4*, 13938–13948. [[CrossRef](#)]
107. Arges, C.G.; Wang, L.; Parrondo, J.; Ramani, V. Best practices for investigating anion exchange membrane suitability for alkaline electrochemical devices: Case study using quaternary ammonium poly(2,6-dimethyl 1,4-phenylene)oxide anion exchange membranes. *J. Electrochem. Soc.* **2013**, *160*, F1258–F1274. [[CrossRef](#)]
108. Nuñez, S.A.; Hickner, M.A. Quantitative <sup>1</sup>H NMR analysis of chemical stabilities in anion-exchange membranes. *ACS Macro Lett.* **2013**, *2*, 49–52. [[CrossRef](#)]
109. Parrondo, J.; Wang, Z.; Jung, M.-S.J.; Ramani, V. Reactive oxygen species accelerate degradation of anion exchange membranes based on polyphenylene oxide in alkaline environments. *Phys. Chem. Chem. Phys.* **2016**, *18*, 19705–19712. [[CrossRef](#)] [[PubMed](#)]
110. Ye, Y.; Elabd, Y.A. Chemical stability of anion exchange membranes for alkaline fuel cells. In *Polymers for Energy Storage and Delivery: Polyelectrolytes for Batteries and Fuel Cells*; American Chemical Society: Washington, DC, USA, 2012; pp. 233–251. [[CrossRef](#)]
111. Danks, T.N.; Slade, R.C.T.; Varcoe, J.R. Alkaline anion-exchange radiation-grafted membranes for possible electrochemical application in fuel cells. *J. Mater. Chem.* **2003**, *13*, 712–721. [[CrossRef](#)]
112. Sata, T.; Yamane, Y.; Matsusaki, K. Preparation and properties of anion exchange membranes having pyridinium or pyridinium derivatives as anion exchange groups. *J. Polym. Sci. Part A Polym. Chem.* **1998**, *36*, 49–58. [[CrossRef](#)]
113. Ameduri, B. From Vinylidene Fluoride (VDF) to the Applications of VDF-Containing Polymers and Copolymers: Recent Developments and Future Trends <sup>†</sup>. *Chem. Rev.* **2009**, *109*, 6632–6686. [[CrossRef](#)] [[PubMed](#)]
114. Neagu, V.; Bunia, I.; Plesca, I. Ionic polymers VI. Chemical stability of strong base anion exchangers in aggressive media. *Polym. Degrad. Stab.* **2000**, *70*, 463–468. [[CrossRef](#)]
115. Ross, G.; Watts, J.; Hill, M.; Morrissey, P. Surface modification of poly(vinylidene fluoride) by alkaline treatment part 2. process modification by the use of phase transfer catalysts. *Polymer* **2001**, *42*, 403–413. [[CrossRef](#)]

116. Merle, G.; Wessling, M.; Nijmeijer, K. Anion exchange membranes for alkaline fuel cells: A review. *J. Membr. Sci.* **2011**, *377*, 1–35. [[CrossRef](#)]
117. Couture, G.; Alaaeddine, A.; Boschet, F.; Ameduri, B. Polymeric materials as anion-exchange membranes for alkaline fuel cells. *Prog. Polym. Sci.* **2011**, *36*, 1521–1557. [[CrossRef](#)]
118. Hagesteijn, K.F.L.; Jiang, S.; Ladewig, B.P. A review of the synthesis and characterization of anion exchange membranes. *J. Mater. Sci.* **2018**, *53*, 11131–11150. [[CrossRef](#)]
119. Fujimoto, C.; Kim, D.-S.; Hibbs, M.; Wroblewski, D.; Kim, Y.S. Backbone stability of quaternized polyaromatics for alkaline membrane fuel cells. *J. Membr. Sci.* **2012**, *423–424*, 438–449. [[CrossRef](#)]
120. Mohanty, A.D.; Tignor, S.E.; Krause, J.A.; Choe, Y.-K.; Bae, C. Systematic alkaline stability study of polymer backbones for anion exchange membrane applications. *Macromolecules* **2016**, *49*, 3361–3372. [[CrossRef](#)]
121. Hickner, M.A. Strategies for developing new anion exchange membranes and electrode ionomers. *Electrochem. Soc. Interface* **2017**, *26*, 69–73. [[CrossRef](#)]
122. Park, E.J.; Kim, Y.S. Quaternized aryl ether-free polyaromatics for alkaline membrane fuel cells: Synthesis, properties, and performance—A topical review. *J. Mater. Chem. A* **2018**, *6*, 15456–15477. [[CrossRef](#)]
123. Amel, A.; Zhu, L.; Hickner, M.; Ein-Eli, Y. Influence of sulfone linkage on the stability of aromatic quaternary ammonium polymers for alkaline fuel cells. *J. Electrochem. Soc.* **2014**, *161*, F615–F621. [[CrossRef](#)]
124. Choe, Y.-K.; Fujimoto, C.; Lee, K.-S.; Dalton, L.T.; Ayers, K.; Henson, N.J.; Kim, Y.S. Alkaline stability of benzyl trimethyl ammonium functionalized polyaromatics: A computational and experimental study. *Chem. Mater.* **2014**, *26*, 5675–5682. [[CrossRef](#)]
125. Barbir, F. *PEM Fuel Cells: Theory and Practice*; Academic Press: Cambridge, MA, USA, 2013.
126. Eriksson, B.; Grimler, H.; Carlson, A.; Ekström, H.; Lindström, R.W.; Lindbergh, G.; Lagergren, C. Quantifying water transport in anion exchange membrane fuel cells. *Int. J. Hydrogen Energy* **2019**, *44*, 4930–4939. [[CrossRef](#)]
127. Grew, K.N.; Ren, X.; Chu, D. Effects of temperature and carbon dioxide on anion exchange membrane conductivity. *Electrochem. Solid-State Lett.* **2011**, *14*, B127–B131. [[CrossRef](#)]
128. Grew, K.N.; Chiu, W.K.S. A dusty fluid model for predicting hydroxyl anion conductivity in alkaline anion exchange membranes. *J. Electrochem. Soc.* **2010**, *157*, B327–B337. [[CrossRef](#)]
129. Takaba, H.; Hisabe, T.; Shimizu, T.; Alam, M.K. Molecular modeling of OH<sup>−</sup> transport in poly(arylene ether sulfone ketone)s containing quaternized ammonio-substituted fluorenyl groups as anion exchange membranes. *J. Membr. Sci.* **2017**, *522*, 237–244. [[CrossRef](#)]
130. Wang, M.; Xu, N.; Fu, J.; Liu, Y.; Qiao, J. High-performance binary cross-linked alkaline anion polymer electrolyte membranes for all-solid-state supercapacitors and flexible rechargeable zinc–air batteries. *J. Mater. Chem. A* **2019**, *7*, 11257–11264. [[CrossRef](#)]
131. Kreuer, K.-D.; Jannasch, P. A practical method for measuring the ion exchange capacity decrease of hydroxide exchange membranes during intrinsic degradation. *J. Power Sources* **2018**, *375*, 361–366. [[CrossRef](#)]
132. Li, N.; Leng, Y.; Hickner, M.A.; Wang, C.-Y. Highly stable, anion conductive, comb-shaped copolymers for alkaline fuel cells. *J. Am. Chem. Soc.* **2013**, *135*, 10124–10133. [[CrossRef](#)] [[PubMed](#)]
133. Ponce-González, J.; Whelligan, D.K.; Wang, L.; Bance-Soualhi, R.; Wang, Y.; Peng, Y.; Peng, H.; Apperley, D.C.; Sarode, H.N.; Pandey, T.P.; et al. High performance aliphatic-heterocyclic benzyl-quaternary ammonium radiation-grafted anion-exchange membranes. *Energy Environ. Sci.* **2016**, *9*, 3724–3735. [[CrossRef](#)]
134. Ziv, N.; Dekel, D.R. A practical method for measuring the true hydroxide conductivity of anion exchange membranes. *Electrochem. Commun.* **2018**, *88*, 109–113. [[CrossRef](#)]

